NOTICE: this is the author's version of a work that was accepted for publication in Sedimentary Geology. Changes resulting from the publishing process, such as peer review, editing, corrections, structural formatting, and other quality control mechanisms may not be reflected in this document. Changes may have been made to this work since it was submitted for publication. A definitive version was subsequently published in Sedimentary Geology, 216, 29-47 (2009). doi:10.1016/j.sedgeo.2009.01.008

Record of Cenozoic sedimentation from the Amanos Mountains, Southern Turkey: implications for the inception and evolution of the Arabia-Eurasia continental collision

Sarah J. Boulton

School of Earth, Ocean and Environmental Sciences, University of Plymouth, Drakes Circus, Plymouth,PL4 8AA, UK.

E-mail - sarah.boulton@plymouth.ac.uk; fax: 01752 233117

Abstract

The sedimentary succession of the southern Amanos Mountains, bordering the eastern margin of the Karasu Rift in south central Turkey, provides a record of environmental change from the Eocene (Lutetian) to the Upper Miocene (Tortonian) that charts the final evolution of the northern margin of the Arabian plate prior to and during continental collision. Eocene shallow-marine carbonates (Hacıdağı Formation) are interpreted as the youngest unit of the Arabian passive margin succession deposited on a northwards facing carbonate ramp. Subsequent deformation and uplift took place during the Oligocene represented by folding of the Eocene and older strata. This is interpreted to be the result of initial continental collision between Arabia and Eurasia. Unconformably overlying the Eocene limestone are Lower Miocene conglomerates, sandstones and palaeosols up to 150 m thick (Kıcı Formation). These were deposited in a range of marginal marine settings consisting of alluvial fan/fan delta facies, flood plain as well as basinal facies. Subsequently, during the Middle Miocene, local patch reefs developed in restricted areas (Kepez Formation) followed by Upper Miocene sediments (Gökdere Formation) composed of relatively deep water hemipelagic marl, with clastic interbeds, which represent a transgression during this period. The Upper Miocene becomes sandier upwards, this records the regression from the relatively deep water facies to coastal sediments. Water depth gradually became shallower until during Pliocene time the area became continental in nature. By the Quaternary rifting had resulted in the development of the Karasu Rift with active alluvial fans along the margins and braided rivers depositing coarse conglomerates in the axial zone. These conglomerates are interbedded with basaltic lava flows that resulted from the region extension across the area. This research shows that initial continental collision occurred in this area after the Lutetian (40.4 Ma) and before the Aquitanian (23.03 Ma) supporting the hypothesis that the southern Neotethys Ocean closed during the Late Eocene to Oligocene. This was a time of climatic change including the onset of southern hemisphere glaciation, in which the closure of the southern Neotethys may have had played an important role.

Key words: Neogene, carbonate ramp, alluvial fan, continental collision, Dead Sea Fault, Neotethys, Eocene-Oligocene boundary.

Cite as: Boulton, S. J., 2009. Record of Cenozoic sedimentation from the Amanos Mountains, Southern Turkey: implications for the inception and evolution of the Arabia-Eurasia continental collision. Sedimentary Geology. 216, 29-47. doi:10.1016/j.sedgeo.2009.01.008

1 Introduction

It is now generally accepted that the geology of southern Turkey records evidence for the evolution and closure of the Southern Neotethys Ocean and the timing of the collision between

Arabia and Anatolia (Sengor and Yilmaz, 1981; Robertson and Dixon, 1984; Yılmaz et al., 1993; Robertson, 2000; Robertson et al., 2004; Robertson et al., 2006). However, there is still much debate on when the northward subduction of Arabia beneath Anatolia ceased and when the closure of the southern Neotethys and subsequent continental collision actually took place (Hall, 1976; Aktaş and Robertson, 1984; Yılmaz et al., 1993; Beyarslan and Bingöl; 2000). There are three main alternative theories, with collision occurring either during: 1) the Late Cretaceous (Karig and Kozlu, 1990; Kozlu 1997; Beyarslan and Bingöl, 2000); 2) in the Late Eocene (Vincent et al., 2007; Allen and Armstrong, 2008) or 3) during the Oligocene to Early Miocene (Aktaş and Robertson, 1984; Yılmaz et al., 1993; Robertson, 2000; Robertson et al., 2004; Robertson et al., 2006) along a suture that runs through SE Turkey (Bitlis Suture; Fig. 1) and into Iran (Zagros Suture; Fig. 1).

The Tertiary evolution of the northern margin of the southern Neotethys has attracted much attention (e.g. Hall, 1976; Aktaş and Robertson, 1984; Yılmaz et al., 1993; Beyarslan and Bingöl, 2000; Robertson, 2000; Robertson et al., 2004; Robertson et al., 2006), but there has been less focus on the coeval evolution of the Arabian margin in the west. Research has been carried out on Cenozoic sediments found within the Bitlis suture zone. These sediments are thought to have been deposited within basins assumed to be representative either of a peripheral foreland basin (Şengör and Yılmaz, 1981; Kelling, 1987) or of small transtensional basins (Karig and Kozlu, 1990; Kozlu, 1997). Additionally, there is some work focussing on the evolution and role of Cenozoic basins on the Arabian platform that are today > 100 km from the suture zone (Hatay Graben, Turkey; Boulton et al., 2006; Boulton and Robertson, 2007: Nahr El-Kabir half-graben, Syria; Hardenberg and Robertson, 2007). Conversely, much of the work on the Arabian margin has concentrated on the Zagros region in Iran and Iraq, 1000s of kilometres to the east (Hessami et al., 2001; Agard et al., 2005; Vincent et al., 2005) and therefore, may not be representative of regions to the west if continental collision was diachronous.

In this paper, I will present the first modern descriptions and interpretation of the Eocene to Late Miocene sedimentary sequence from the southern end of the Amanos Mountains, ~ 50 km south of the suture zone (Figs. 1, 2). This study focuses on the area around the towns of Kırıkhan, Belen and Serinyol in the Hatay Province of southern Turkey where Cenozoic strata outcrop in the Amanos Mountains due to uplift on the flanks of the Plio-Quaternary Karasu Rift. New sedimentological and petrological data are presented for these rocks based upon a recent redefinition of the stratigraphic framework (Boulton et al., 2007). This allows new palaeoenvironmental interpretations to be made and implications drawn for the palaeogeographic evolution of the northern Arabian plate margin during the final stages of continental collision and the subsequent development of a peripheral foreland basin on the Arabian plate.

2 Geological Framework

The DSFZ system forms the boundary between Arabia and Africa (Fig. 1), accommodating the difference in motion between the two plates through sinistral strike-slip motion. The DSFZ trends ~ N-S from the Red Sea, in the south, to the junction with the East Anatolian Fault Zone (EAFZ) near Kahramamaraş in southern Turkey, in the north. The DSFZ developed, in the south, during the Middle Miocene (dated as <20 Ma, Lyberis, 1988; 18 Ma, Garfunkel and Ben Avraham, 1996) with the slip rate calculated as ~7 mmyr^{-1} (Garfunkel et al., 1981).

The Karasu Rift forms the northernmost segment of the Dead Sea Fault Zone (DSFZ), located primarily in the Hatay Province of Turkey, trending northwards from the Amik Plain (Fig. 1). To the south of the Amik Plain, the Gharb Rift forms the southwards continuation of the DSFZ; while to the east another structure, the Hatay Graben, trends NE-SW to the present Mediterranean coast. The Karasu Rift can be subdivided into three segments (Rojay et al., 2001); northern, central and southern. This paper will focus on the western margin of the southern segment of the Karasu Rift from Kırıkhan in the north to Serinyol in the south.

The Karasu Rift is bounded by two main faults the Amanos Fault Zone (AFZ) in the west and the East Hatay Fault (EHF) in the east (Fig. 1). Slip rate estimates of the AFZ from offset lavas range from 0.3 $mmyr^{-1}$ (Arger et al., 2000, based upon data from Çapan et al., 1987), 2 – 15 $mmyr^{-1}$ (Rojay et al., 2001), 1 – 1.6 $mmyr^{-1}$ (Yurtmen et al., 2002) to 4 $mmyr^{-1}$ (Tatar et al., 2004). There are few estimates for the slip rates of the EHF, amongst which those of Tatar et al., (2004) who derived a figure of 4 $mmyr^{-1}$ for the EHF. Although motion on these faults is dominantly sinistral strike-slip there is a normal component of motion that has lead to the development of the Karasu Rift and, which caused the uplift of the Amanos Mountains to the west of the rift. The Amanos Mountains are composed of a core of metamorphosed Precambrian rocks, Palaeozoic sediments, ophiolite and Cenozoic sedimentary cover, whereas the rift fill is poorly exposed recent alluvium with interbedded lavas (Fig. 2).

Pioneering geological research in the study area was undertaken by Dubertret (1939, 1953), followed by the first subdivision of the Palaeozoic rocks of the Amanos Mountains by Dean and Krummenacher (1961) and of the complete stratigraphic sequence by Atan (1969). Geological mapping of the Amanos Mountains as a whole was undertaken by Schwan (1971), Ishmawi (1972), Janetzko (1972) and Lahner (1972) but these works generally lacked widespread correlation and palaeontological age constraints. The 1980s saw an increased interest in the area by the Turkish Petroleum Corporation (detailed list in Dean et al., 1986). Although the majority of this work is still unpublished, the work of Guney (1984) presents important micropalaeontological biozonation of Cenozoic formations. Piskin et al., (1986) published a new geological map for the Hatay region, with a brief synopsis of the sedimentary units based mostly on the earlier work of Atan (1969). In the same year, Dean et al., (1986) presented a revised stratigraphic scheme for the Palaeozoic sediments of the southern Amanos area (around Kırıkhan), which did not include the Cenozoic stratigraphy. Further geological mapping in the Kırıkhan and Belen areas was undertaken by Kop (1996) and Dokumaci (1997).

It is evident that the sedimentary cover has only received rudimentary attention, in comparison to the detailed analysis and interpretation of the Upper Cretaceous ophiolite (e.g., Çogulu, 1974; Delaloye et al., 1980; Piskin et al., 1986), the structural geology of the Karasu Rift (e.g., Saroglu et al., 1992; Rojay et al., 2001; Westaway and Arger, 2001; Adiyaman and Chorowicz, 2002; Over et al., 2002; Yurtmen et al., 2002; Westaway, 2003; Tatar et al., 2004; Akyuz et al., 2006) and the nature of the Karasu basalts (Çapan et al., 1987; Parlak et al., 1998; Rojay et al., 2001; Yurtmen et al., 2002; Tatar et al., 2004).

3 Cenozoic sediments of the Karasu Rift

The Cenozoic sediments of the Southern Karasu Rift (Table 1) occur predominantly around the towns of Kırıkhan, on the western edge of the Karasu Rift, and Belen in the Amanos Mountains (Fig. 2). The strata range from Eocene to Late Miocene in age, the Eocene strata are folded and faulted (Boulton and Robertson, 2008) and unconformably overlain by relatively undeformed Neogene sedimentary rocks. This sedimentary cover overlies the Hatay/Kızıldağ Ophiolite that was emplaced southwards during the Maastrichtian (Robertson, 2002). A smaller outcrop of Cenozoic-aged sediment is preserved on the edge of the Amik Plain around the town of Serinyol, to the north of Antakya and southwest of Kırıkhan. This area lies in the southernmost part of the Karasu Rift within a re-entrant of the ophiolite. A sequence of Palaeocene-Eocene to Upper Miocene sedimentary rocks is exposed in this small area (Fig. 3). In this section sedimentary descriptions and interpretations of the Cenozoic units are given, which are then used to build a model of palaeogeographic change in the study area allowing comparisons to other areas and an evaluation of major tectonic events.

3.1 Eocene limestone - Hacıdağı Formation.

There are large exposures of Eocene limestone along the Belen and Kırıkhan roads to Antakya. The limestone (Hacıdağı Formation) varies from fine-grained wackestone and packstone to rudstone. Bedding is thin (0.1-0.2 m thick) with sharp bases and tops and often normally graded, bases of some beds are erosional and many are laterally discontinuous. Additionally, bedding is disrupted in places where slumping has occurred or was incipient (Figs. 4a, b). Data from fold hinges and bedding in slumped horizons indicates a general ~ 000° - 020° for the down-slope direction (Fig. 5). Planar lamination is common, and there is abundant bioturbation, where burrows can be seen to cut and disrupt the laminations in some beds. There are numerous large benthic foraminifera, often concentrated in lags at the bases of the beds. Planktic foraminifera are also reported from these limestones such as *Globorotalia velascoensis* (Cushman), but benthic species are the most diverse (*Nummulites* sp., *Discocyclina* sp., *Orbitolites* sp., *Alveolina* sp., *Assilina* sp. (Atan, 1969)) dating the formation to the Lutetian (Boulton et al., 2007). Chert is common, forming dark grey to black, elongated nodules parallel to the bedding planes. Occasionally there are horizons of angular- to well-rounded clasts, composed of limestone and serpentinite. Overlying these thinly bedded limestones is a laterally extensive bed, ~10 m thick, that has an erosive base. This is a matrix-supported conglomerate with sub-rounded clasts of fine-grained, white limestone (< 70 mm) in a matrix of non-fossiliferous white nummulitic wackestone/floatstone.

Along the Belen-Antakya road section, the basal contact between the Hacıdağı Formation and the underlying ophiolite (sheeted dyke complex) is generally sharp and does not appear to have any basal conglomerate or other lithological changes associated with it, and is therefore interpreted as a faulted contact. The upper boundary of the formation can be observed on the main road just before Belen. The top of the Eocene limestone is eroded and bedding is sub-vertical. Overlying basal Miocene sediments contain well-rounded clasts of Eocene limestone indicating an erosional contact.

Eocene limestones are also exposed along a riverbed near Serinyol (Fig. 6b). Here the formation (Fig. 3) directly overlies the eroded upper surface of the ophiolite, along a disconformity. The base of the sequence is composed of hard white limestone (wackestone-packstone) containing large benthic foraminifera (*Nummulites, Discocyclina)* and common chert nodules. Within this basal limestone there is a large, laterally discontinuous, conglomerate horizon (Fig. 4c), the base of which is irregular and cuts down to the top of the ophiolite in the north. This conglomerate is poorly sorted and clast supported, composed entirely of sub-angular to sub-rounded, limestone and chert clasts (Table 1) up to 0.9 m in size. The matrix is sandy and contains *Amphistegina* sp., *Operculina* sp., *Rotalia viennotti*, *Quinqueloculina* sp., *Globigerina* sp., *Miogypsina* sp., *Textularia* sp., *Lepidocyclina* sp., and unidentifiable foraminifera of the Rotaliina. There are also fragments of *Lithophyllum*.

Above the conglomerate, there is a return to limestone (fine-grained sparite). Bedding is thin and irregular; the upper surfaces of the beds occasionally exhibit current ripples. Chert nodules are very common and *Nummulites* and other large benthic foraminifera are occasionally observed in dense accumulations. Within this sequence there are several clast supported conglomerate horizons; the clasts are angular to sub-rounded, <0.5 m in size and composed of limestone and chert. There is also a thick (2.5 m) rudstone bed that has an irregular base that cuts down into the underlying beds. *Nummulites* and *Discocyclina* exhibit a rough parallel alignment. Additionally, there is a small change in bedding orientation above and below this bed.

A conglomerate horizon is observed near the abandoned village of Kanlidere (Fig. 6a). Thin-bedded, wackestone with chert nodules is exposed in the valley bottom. The top of the formation is a 7-10 m thick, clast-supported conglomerate, clasts are sub-angular to sub-rounded composed of limestone and chert (Table 3), with a maximum clast size of 0.3 m. Although generally poorly sorted there are horizons within the conglomerate that exhibit better sorting.

3.1.1 Interpretation

The characteristic planar beds, which fine-upwards and exhibit parallel lamination, suggest that these limestones were deposited from low density turbidity currents consisting of the T_{abe} divisions of the classical Bouma sequence (Bouma, 1962). The T_{cd} divisions of the Bouma sequence are generally absent, suggesting that partial flow separation may have taken place resulting in incomplete sequences.

Some horizons are distorted and broken; these were interpreted as incipient slumps as the bedding was broken but significant offset in the bedding planes had not occurred (Fig 4a). Other horizons show more obvious evidence of slumping including a spectacular isoclinal fold (Fig. 4b). The orientation of these structures indicates the presence of a northward-dipping slope (Fig. 5). The thin-bedded facies are commonly capped by a thick bed of laterally extensive, matrix-supported conglomerate. The clast size, shape and overall texture suggest the conglomerate was probably lain down by a powerful a debris flow (Nilsen, 1982).

Poorly sorted, clast-supported conglomerates were observed at Serinyol and Kanlidere (Fig. 6). The clast-supported nature suggests deposition was not by a debris-flow process but that it was deposited from a hyperconcentrated sediment flow. In addition, several conglomerate horizons are present near Serinyol. The main conglomerate bed cuts out the basal part of the underlying bedded Eocene limestone and sits directly on top of the underlying ophiolite. It is probable that this conglomerate represents a channel fill; however, it was not possible to determine the channel orientation. Foraminifera identified in the matrix indicate derivation from a shelf environment. Near the top of the sequence there is a widespread but slight angular (1-2°) discordance within the formation, directly below this there is a thick bed of Nummulitic rudstone with an erosive base; this may be the result of scouring, possibly following a tectonic event. Only one conglomerate horizon was observed at Kanlidere. The lenticular nature of these clast-supported conglomerates suggests that these could be channel-fill deposits or scour fills.

The abundance of large benthic foraminifera and low abundance of planktic forms indicates relatively shallow water depths. The presence of *Nummulites* sp., in particular indicates water depths of 20 – 75 m (Saller et al., 1993) although reworking to deeper water is likely as the foraminifera are often found in concentrated lags.

Therefore, the biotal evidence combined with evidence for sediment instability and movement (slumps, turbidites and channel fills) suggests that during the Eocene in this northern area, carbonates were being deposited on a slope, orientated approximately northwards. The slope was unstable generating debris flows and turbidity currents and was cut into by large channels that were in-filled by coarse-grained sediments.

3.2 Lower Miocene sandstone and conglomerates - Kıcı Formation.

The base of the Kıcı Formation rests unconformably on the Eocene at the type section near Kurtisoguksu (K; Fig. 2); as is the case throughout the area as Oligocene sediments are absent. A thick-bedded, dominantly matrix-supported conglomerate unit, 50-60 m thick, is present at the base of the section (Fig. 7). Clasts are up to 1 m in size, angular to sub-rounded and composed dominantly of carbonate, although there are some basaltic and red sandstone (probably from the underlying Palaeozoic strata) clasts present. Above this basal conglomerate there is a sequence of coarse-grained purplish-red sandstone. Beds are 0.3-3 m thick with sharp bedding plane contacts. Grain-size is generally very coarse but also conglomeratic and mudstone horizons are present. Sandstone beds often exhibit normal grading, contain "floating" rounded pebbles (< 20 mm in general) and pebble stringers that contain predominately serpentinite clasts (derived from the underlying ophiolite). In general, serpentinite is the main constituent of the sandstones in the Kıcı Formation (Table 3). Sedimentary structures are common, such as parallel lamination, planar cross-bedding (< 0.1 m high foresets) and bioturbation (Fig. 8). It should be noted however, that reliable palaeocurrent measurements could not be determined due to the poor nature of the exposure.

Conglomerate beds are clast-supported, with well-rounded clasts of a generally ophiolitic composition; rare limestone clasts are also present. The conglomerates are either found at the base of sandstone beds or form laterally discontinuous lenses. There is also an interval with 1.75 m of mudstone exposed. The bottom 1 m is composed of thin interbeds of white and pale lilac-coloured chalk and black mudstone, which is overlain by dark grey mudstone containing roots and plant material.

The Lower Miocene succession is also observed to overlie the Eocene limestones above an erosional unconformity near Gökdere (Fig. 4d); however, no basal conglomerate is present at this location, only 1.5 m of mixed breccia and red mudstone (Fig. 9). Above this there is ~5 m of coarse-grained boundstone, composed mostly of large fragments of algal material (Rhodophyta;

Lithophyllum sp., *Corallina* sp.: Dasycladaceae; *Halimedia* sp.), other bioclastic (Foraminifera; *Textularia* sp., *Spiroloculina* sp., *Globigerina* sp., *Amphistegina* sp., *Quinqueloculina* sp., *Triloculina* sp., *Globorotalia* sp., including *G. menardii*, *Rotalia viennotti* and *Miogypsina* sp) and some siliciclastic material. Upwards, the sequence is dominated by coarse litharenite and conglomerate. Conglomerates are matrix-supported and composed of rounded clasts of dominantly ophiolite material (Table 2). Limestone clasts are also present, which occasionally show evidence of boring. Clasts are well-rounded and the size varies between beds. Rounded “floating” pebbles are very common within the sandstone beds.

Higher in the section, sedimentary structures become more common and parallel lamination, trough and planar cross-bedding, pebble imbrication and bioturbation are present. Although, current indicators are present most are unsuitable for measurement, three measurements on imbricate pebbles were measured (080°, 090°, 120°) suggesting an easterly flow. Additionally, there are occasional mudstone beds, generally black in colour with a shaley fabric, with abundant plant material and rootlets in some horizons. The top of the sequence is poorly exposed but it appears that there is an upward transition to the overlying Kepez Formation. The coarse litharenite is light purple to red due to the high content of altered serpentinite. Thin-sections reveal that basaltic clasts and polycrystalline quartz are also common.

To the southwest, at Kanlidere, the Lower Miocene is markedly different, there ~40 m of Lower Miocene sediments outcrop. Fine- to medium-grained, poorly sorted, massive brown sandstone is exposed (Fig. 6a), containing unidentified gastropods, fragmented and reworked *Corallina* sp and *Lithophyllum* sp., algae, and some foraminifera (*Triloculina* sp., *Neoalveolina* sp., *Spiroloculina* sp., and unidentified Rotaliina). Interbedded with the massive sandstone there are three conglomerate horizons (Fig. 6a). These conglomerates are clast-supported, poorly sorted with well-rounded to sub-rounded clasts up to 0.4 m in size (Fig. 10a). The matrix is composed of fine-grained, brown sandstone, similar to the rest of the exposure and the clasts have a mixed composition of limestone and ophiolite (Table 2). Many of the limestone clasts exhibit *Lithophaga*-

like borings. The top of the formation is conformable with the overlying limestone (Middle Miocene Kepez Formation).

The Lower Miocene, near Serinyol, is different again. The sediments here are composed of 30 - 40 m of red and brown mottled mudstones with abundant caliche nodules and palaeosol horizons (Fig. 6b). However, individual beds cannot be distinguished due to the heavily weathered and diagenetically altered nature of the sediments. No conglomerate was observed in this section.

3.2.1 Interpretation

Although there is no dating evidence for this formation, the stratigraphic position below the Kepez Formation suggests an Early Miocene age and foraminifera identified in the basal bioclastic facies observed at Gökdere, confirm a Miocene age for the base of the formation. The sedimentary characteristics of the Kıcı Formation can be broadly differentiated into three facies associations; alluvial fan, braided stream and shoreline.

The presence of both matrix- and clast-supported conglomerates at the base of the type section, is suggestive of both debris-flow and sheet flood processes. Using standard nomenclature (Miall, 1978; 1985; 1996) these sediments can be classified as Gmm and Gcm facies, indicating a SG facies association, interpreted as coarse alluvial fan sediments. The disorganised fabric, large clast sizes and matrix-supported intervals indicate deposition on a debris flow dominated alluvial fan (Postma, 1986; Blair and McPherson, 1994). There is no fossil material present, consistent with a non-marine origin.

In contrast, the basal sediments consisting of 1.5 m of breccia and palaeosols at Gökdere, probably formed through exposure and weathering of the underlying limestone. This is overlain by microbial boundstone; fossil content indicates a shallow-marine origin for this material with some reworking and abrasion causing fragmentation of the bioclasts. The encrusting nature of the Rhodophyta (red algae) caused biological binding of the carbonate and suggests a high-energy shallow-marine setting (Wright and Burchette, 1996), such as the edge of an algal reef.

The upper part of the Lower Miocene is composed of conglomerate and coarse litharenites with occasional mudstone horizons. However, the type section is a fining-upwards sequence (Fig. 7), whereas a coarsening-up sequence is identified at Gökdere (Fig. 9). Conglomerate horizons generally occur at the base of sandstone beds or as laterally discontinuous lenses at the type section. By contrast, there is a higher proportion of conglomerate present at Gökdere. The limestone clasts locally show evidence of *Lithophaga*-like boring, indicating that some pebbles were reworked in a shallow marine setting before being incorporated into the these conglomerates, as *Lithophaga* sp. live in the littoral zone of marine coasts.

The cross-bedded sandstones with basal lags of conglomerate seen at the type location are suggestive of lateral and downstream accretion macroforms and possibly sandy bedforms, suggesting possible deposition from a braided coarse-grained to sandy bedload river (Miall, 1996). The fine-grained sediments consisting of soft dark grey to black mudstone indicates high organic matter content indicative of water-logged conditions. The presence of rootlets and plant material suggests non-marine conditions and colonisation by plants, indicating deposition on a flood plain, abandoned channel, or marsh adjacent to the active channel.

By contrast, the sandstone exposed at Kanlidere contains bioclastic material including coralline algae, gastropod and bivalve fragments, and both benthic and planktic foraminifera, indicating a marine (possibly a shallow-marine peri-reefal) environment. The massive nature of the sandstone suggests that it has undergone intense bioturbation. Three clast-supported conglomerate beds are interbedded with the sandstone (Fig. 6a), suggesting a stream-flow or tractional reworking and winnowing and deposition in a coastal setting. Some of the limestone clasts have borings, also indicating reworking in a shallow-marine environment prior to deposition. The features described in these sediments may indicate deposition in the lower shoreface. The mudstones near Serinyol, interpreted as a palaeosol succession (Fig. 6b), indicate this area was emergent and undergoing soil formation during the Early Miocene.

In addition to the shoreface deposits at Kanlidere, there is evidence of marine influence (i.e. basal boundstone) at Gökdere, suggesting that this location was proximal to the coast unlike the type section and represents a regressive sequence. This could imply that these locations represent a lateral transition of alluvial fan-braided/meandering river-deltaic environments. Therefore, these facies associations indicate a range of depositional environments along a coarse-grained gravel rich coast as evidenced by the interaction of marine and alluvial processes. This coarse-grained coast appears to evolve over time from an alluvial fan delta to a braid delta (Orton, 1988) reflecting the change in the feeder system from a point sourced alluvial fan to a braided river system (feeder system types A and B of Postma, 1990). It is not clear whether this fan-delta system is a low gradient shelf-type, shallow water delta or a slope-type, deep water delta (Postma, 1990) as the pro-delta sediments have not been identified.

The composition of the sandstone of the Kıcı Formation is dominated by serpentine, basalt and radiolarian chert clasts and there is very little matrix or cement present. This indicates that the sediment source was probably the underlying ophiolite and related rocks. In contrast, the conglomerate horizons at Kanlidere were dominantly derived from the sedimentary cover (mainly limestone and chert). Fine-grained sediments contain abundant quartz and muscovite; these minerals could be extrabasinal as mica, especially, is uncommon in the local basement rocks.

3.3 Middle Miocene - Kepez Formation: limestone.

The Kepez Formation is poorly exposed only at a few locations. Near Kepez Hill (adjacent to Gökdere village), the Middle Miocene is a small exposure of rubbley limestone. This is composed of shallow-marine debris, such as fragments of oncolite, coral, bivalves, gastropods and echinoids. Additionally, a large amount of coralline (mainly poritid corals) debris is strewn about the hillside in this area.

Near Kırıkhan, there is a small outcrop of fine-grained crystalline wackestone containing fragmented coralline algae, foraminifera and echinoids. This bed is variable in thickness (2-3 m) and has an uneven basal surface. This overlies an extremely poorly exposed soft marly limestone. By contrast, 10-15 m of Middle Miocene limestone is well exposed at Kanlidere (Fig. 6a). The basal beds are marly wackestone and pass upwards into hard packstone. There is abundant bioclastic debris, bivalve fragments, bryozoa, echinoids, small gastropods, coral and oncolites.

The Middle Miocene exposure near Serinyol is irregular and of a variable thickness (2 to 6 m) composed of recemented rubbley material. Blocks are ~10cm in size, angular and clast-supported. The limestone is rich in bioclastic material, such as *Pecten*, *Ostrea*, poritid corals and gastropods (Fig. 10b). Underlying this material there is an irregular basal bed of limestone rich in fragmented bivalves.

3.3.1 Interpretation

These limestones are very poorly exposed and the bioclastic material is fragmented; therefore, there is little information on which to base an environmental reconstruction. Generally, the bioclastic packstone indicates formation in shallow-marine conditions, which possibly accumulated slightly offshore as the fragmentation of the bioclastic material indicates that it was reworked. Also, the large blocks of limestone seen in the north are characteristic of reef talus.

The large coral fragments and the rubbley nature of the limestone, near Serinyol, indicate that this may also be reef talus, confirming the presence of shallow-marine reefs. As this facies is observed in a number of different locations (Fig. 3) and as large fringing reefs are uncommon in the Mediterranean during the Miocene (Franseen et al., 1996), it is most likely that this material was derived from small patch reefs.

3.4 Upper Miocene mudstone with sandstone interbeds - Gökdere Formation.

The type section of the Upper Miocene at Gökdere is composed of fine-grained, grey marl (Figs. 10c, 12; Table 4). Near the base of the formation are thin (50 mm) interbeds of fine-grained micaceous litharenite (Table 3). Some of these thin beds exhibit parallel laminations and contain plant fragments, small gastropods and ostracods, but marl sampled for faunal studies were barren. Upwards the proportion of sand increases; sandstone beds become thicker (< 0.5 m) and more abundant (Fig. 10d). Sandstone beds are usually found in packets with a significant thickness of marl between. The sandstone is laterally discontinuous with sharp upper and lower bedding surfaces. There are an abundance of sedimentary structures present in the sandstones, including small channel structures, parallel lamination, cross-bedding, ripples, rip-up clasts, load casts, and current-aligned plant material.

The proportion of sand continues to increase upwards until bedding thickness exceeds 1 m; these beds continue to be interbedded with marl. Near the top of the exposed sequence thin micritic carbonate horizons are interbedded with the sandstone and marl (Fig. 11). The sandstone weathers orange and sedimentary structures are uncommon; although mud rip-up clasts and bioturbation were observed. There are many elongate carbonate-cemented concretions. In thin section these massive litharenites are composed of a range of lithic fragments (dominantly serpentinite and limestone clasts), quartz, muscovite, biotite and rare glauconite with some clay matrix and sparry calcite cement. Additionally, there are fragments of transported algal clasts as well as (transported?) planktic (*Globigerina* sp., *Globigerinoides* sp.) and benthic foraminifera (*Amphistegina* sp., and indeterminate Rotaliina). Occasional oyster beds are present, where individual *Ostrea* specimens can exceed 0.2 m in length. *Turitella* gastropods and plant material are present in adjacent beds. Thin carbonate beds exhibit parallel lamination and, in thin-section, layers of disarticulated ostracods valves apparently of only two taxa. The ostracod species are undetermined but *Cyprideis seminulum* (Reuss) and *Cyprideis anatolica* (Bassiovini) have been reported from this formation by Kop (1996).

Around the town of Belen and to the south, the Upper Miocene is well exposed, here composed of interbedded sandstone and marl/mudstone. The mudstone is very fine-grained, variable in colour and forms the majority of the succession. The litharenite/calcarenite is fine- to coarse-grained; beds are normally graded and micaceous. Bed thickness is generally < 0.5 m, but most beds are < 0.1 m thick; laterally, these beds are discontinuous, tending to form discrete packets within the marl. Sedimentary structures are common; parallel laminations, ripples, cross-laminations were all observed. Fallen blocks reveal that the bases of the beds have various sole marks (formed by erosion and bioturbation). Fossils are not generally present but *Ostrea* fragments were identified and plant material is quite common.

The basal Upper Miocene sediments near Serinyol are grey marl, containing small bivalves (undetermined) and foraminifera (*Globigerinoides trilobus* (Reuss); *Orbulina suturalis* (Brönniman); *Orbulina bilobata* (d'Orbigny); Boulton et al., 2007) and also fragments of larger bivalves and polyzoans. Upwards, the colour changes to brownish. There are occasional horizons with parallel laminations but there are no major lithological variations. The upper part of the formation, includes packages of sandstone beds, these are 10-20 m thick and formed from thin, irregular beds of medium-grained calcarenite, separated by a similar thickness of marl. Ripples, planar cross-lamination, tepee structures and rip-up clasts are present. Some fossil material is present, mostly as fragmented bivalves.

Palaeocurrent measurements from this formation were based generally on ripples, sole marks and, at the type section, from flow-oriented plant debris. Although there is some spread in palaeocurrent orientation, in general they indicate a southerly to westerly flow (Fig. 12).

3.4.1 Interpretation

The Upper Miocene forms a coarsening-upward sequence. This sequence is interpreted to represent a progradational shoreline succession, characterised by a shallowing and coarsening-upwards sequence from marine offshore muds to silt and sand facies of the shoreface (Reading & Collinson, 1996). The basal sediments dominated by marl deposition are interpreted as basinal mudstones.

Higher in the succession the proportion of sand increases, probably relating to shallowing and regression. The laterally discontinuous, generally massive beds with erosional bases are likely to be channel fills. Whereas, the more laterally continuous beds that show a wider range of sedimentary structures, such as parallel laminations, cross-lamination, ripples and rip-up clasts, are interpreted as storm generated current deposits due to the similarities to the current-modified turbidite model of Myrow and Southard (1996).

At the type section (Fig. 11), the sequence continues to coarsen upwards and biodiversity is low in some beds with only one species of *Turitella* and occasional large *Ostrea* present. This low diversity fossil assemblage could suggest a stressed, possibly brackish water, environment but may also be the result of the preferential dissolution of aragonite post-deposition. However, the presence of *Ostracoda* probably *Cyprideis* sp., in thin carbonate horizons is indicative of brackish water, lagoonal or lacustrine environments of very shallow water, < 10 m in depth (Neale, 1988). Conversely, a more diverse assemblage, albeit reworked, is found in the massive sandstones indicating that this material was transported from fully marine conditions. These massive beds could have been deposited in the lower shoreface where bioturbation may have obliterated sedimentary structures or again they may be tempestite deposits. Palaeocurrent analysis indicates a general direction of sediment transport to the west/southwest (Fig. 12), suggesting shore-oblique currents consistent with storm generated deposition (Myrow and Southard, 1996).

At locations other than the type section, these upper coarse sandstones and thin carbonate horizons are absent. This may be because erosion has removed the upper part of the Miocene in these other localities or that the shoreline was further into the basin and in the subsurface at the present time.

The marls are composed dominantly of argillaceous lime mud but also contain significant amounts of quartz (Table 4). Quartz is not expected to be present in high volumes if erosion of the underlying ophiolite is the main sediment source. This suggests that some detritus was being sourced from other rocks types, possibly from quartzite exposed in the core of the Amanos Mountains north of Kırıkhan (e.g., Sadan, Sosink, Seydişehir Formations), or from even more distant sources, such as the Taurides. Muscovite is present in some samples from the Kıcı and

Gökdere Formations and is likely to have an extrabasinal source, possibly from metamorphic rocks, as micaceous rocks are not common in the immediate area.

4 Discussion

4.1 Evolution of the north-western Arabian margin

The Hatay (Kızıldağ) and Baer-Bassit Ophiolites were emplaced during the Maastrichtian (Al-Riyami et al., 2002), southwards onto the Arabian margin. Rising eustatic sea-level (Miller et al., 2005) possibly combined with isostatic regional subsidence following ophiolite emplacement resulted in a widespread marine transgression across the Arabian platform throughout Palaeocene and Early Eocene times. Directly to the south of the study area, in the Nahr El-Kabir region of Syria, Early – Middle Eocene limestones (Fig. 13) are characteristic of open-shelf conditions with evidence of westward shallowing during the Middle Miocene (Hardenberg and Robertson, 2007). Similarly, to the southeast of the study area, in the present Hatay Graben, Lutetian sedimentation was characterised by a marine transgression from intertidal to shallow open marine conditions (Boulton and Robertson, 2007). However, in the Belen- Kırıkhan area facies are dominated by turbidites and northward flowing slumps, indicating a depositional position on the outer ramp or ramp slope of the Neotethys margin (Fig. 14a). This field evidence is in agreement with current palaeogeographic models of the region for that time (e.g., Meulenkamp and Sissingh, 2003).

Chert is common in these facies and similar facies have been observed in Eocene carbonates in Hatay, Turkey (Boulton and Robertson, 2007), Syria (Hardenberg and Robertson, 2007), Israel (Rosenfeld and Hirsch, 2005) and onshore and offshore Cyprus (Robertson, 1998). The presence of diagenetic chert is generally attributed to high diatom and radiolarian productivity either due to upwelling on the Neotethys margin (Boulton and Robertson, 2007) or due to a marine connection between the Mediterranean and the Indian Ocean (Hardenberg and Robertson, 2007).

Following the deposition of the Eocene carbonates there was a period during which folding and uplift took place (Boulton and Robertson, 2008). It is likely that this deformation explains the Oligocene hiatus, which formed during the initial continental collision between Eurasia and Arabia. Evidence collected here indicates that the collision took place sometime between the Lutetian (youngest platform carbonates in the area) and the Aquitanian (assumed age of the oldest sediments above the regional unconformity surface). Such deformation has also been recorded for the Hatay basin to the southeast (Boulton and Robertson, 2007) and recognised to north on the conjugate margin seen in the east-central Taurides (Karig and Kozlu, 1990), but was not mentioned by Hardenberg and Robertson (2007) as having effected coeval strata in northern Syria. Interestingly, although strata of Oligocene-age are not present in the study area or in the Hatay Graben, strata from this epoch are present elsewhere to the south, in Syria and Jordan, indicating that the hiatus in sedimentation during the Oligocene was confined to the northernmost margin of the Arabian plate. This may indicate that the collisional front was located near to the present-day Bear-Bassit area of northern Syria. It has also been suggested (Hempton, 1985; Sharland et al., 2004) that non-deposition in these northern areas of the Arabian plate may have resulted from local uplift during reactivation of structural lineaments related to the Syrian Arc, but it may also be significant that the Oligocene was a period of low eustatic sea-level (Miller et al., 2005).

During the Early-Middle Miocene conglomerates and sandstones were deposited (Fig. 14b). Basal sediments were deposited in an alluvial fan setting. Alluvial fans typically form in regions of active deformation where a hinterland with steep relief is separated from a lower relief basin by a rapid change in slope gradient (Heward, 1978). This may indicate the presence of an active fault at this time, but there is no supporting evidence for syn-sedimentary tectonic movement so it is suggested that the fan formed as a result of erosion of mountains rapidly uplifted by initial continental collision. Upwards there is a transition to a braid delta system, which prograded east-south eastwards, into a marine embayment in the Amik Plain area (Fig. 14b). Clast sizes are significantly smaller higher in the section, this decrease through time could be the result of lowered relief. Palaeosols exposed near Serinyol are interpreted as the lateral, terrestrial equivalent to these sediments deposited in a floodplain environment.

The dominant clast lithology of serpentinite in the Kıcı Formatıon indicates that the sediment source was the ophiolite emplaced in the Maastrichtian. However, the presence of limestone clasts identified as being similar to the Eocene facies, indicates that the young carbonates had already been uplifted and were being eroded; this probably took place during the Oligocene. The Kıcı Formatıon can be correlated with Early Miocene braided-river sediments identified in the Hatay basin to the southeast (Balyatağı Formation; Boulton and Robertson, 2007) that flowed northwards from the Baer-Bassit Massif, Syria (Fig. 13). This contrasts with a marine signature for some parts of the Early Miocene sediments in the Kırıkhan area, although a brief marine incursion in the Early Miocene has been recorded from the Hatay basin as well (Boulton and Robertson, 2007). This implies that regionally there was a marine incursion in the earliest Miocene with a regressive trend occurring through the Early and Middle Miocene leading to continental deposition in the Hatay basin and coastal environments to the north.

By contrast, Early Miocene sediments to the north of Kırıkhan, in the suture zone of the orogeny, are significantly different. These are mainly deep water turbidites that thicken southwards (Lice Formation: Aktas and Robertson, 1984; Karig and Kozlu, 1990; Robertson et al., 2004; Gül, 2006). Sole marks in those Aquitanian sediments indicate an easterly flow direction along an east-west orientated basin in the northeast, whereas in the Iskenderun basin the dominant flow direction was to the southwest (Karig and Kozlu, 1990).

To the south at this time the Nahr El-Kabir half graben developed separating the Baer-Bassit Massif in the northeast from the main Arabian shelf to the south and east (Hardenberg and Robertson, 2007). Sedimentation during this time was dominated by marine carbonates (Fig. 13). This indicates that Baer-Bassit, Hatay Basin, Amanos range and parts of the southern Karasu Rift represented a topographic high during the Early Miocene between the shallow marine carbonate platform to the south and the foreland (Lice and Iskenderun Basins) to the encroaching collisional front to the north. This is in agreement with Boulton and Robertson (2007) who proposed that the Early Miocene sediments in the Hatay Basin represented erosion of the flexural forebulge created by tectonic loading of the subducting slab accentuated by reactivation of basement structures.

The Middle Miocene saw the development of localised patch reefs in the study area (Fig. 14c), which pass laterally and vertically up into a coarsening-up sequence of marl to sandstone. The presence of patch-reefs indicates suitable conditions for coral growth; however, these conditions were short lived possibly due to the influx of fine-sediment stifling coral growth. The overlying marl sequence has been dated as Serravallian to Messinian in age (Kozlu, 1982) and the patch reefs as Langhian–Serravallian (Kozlu, 1982). The marls are marine in the south near Serinyol, however, the presence of *Ostrea* sp., *Cyprideis* sp., and *Turitella* sp., suggests a restricted marine to brackish water-environment in the north, at the top of the succession, indicating a shallowing in water depth to the northeast (Fig. 14d).

This sequence shares many similarities to the sediments in the Hatay area, although faulting related to the formation of the Hatay Graben appears to have initiated during the Middle Miocene (Boulton et al., 2006) the area was still part of the wider foreland basin to the thrust front (Boulton and Robertson, 2007). Sedimentation during the Langhian and Serravallian was dominated by shallow-marine peritidal carbonate deepening up into outer ramp carbonates and then marls over time possibly due to flexural subsidence relating to foreland loading (Boulton and Robertson, 2007). Patch reefs were identified in the northwest of that area (near Kesecik, Boulton and Robertson, 2007; their figure 1), close to the area discussed in this paper indicating that the study area was also part of the shallow underfilled foreland basin of the collisional zone. It is possible that subsidence was greater in the southeast due to the effect of local normal faulting superimposed on regional subsidence; whereas the absence of normal faulting in areas to the north reduced overall subsidence rates and the resulting accommodation space.

However, the marls of the Hatay and Karasu sequences differ in composition with higher concentration of quartz and mica present in the sediments around Kırıkhan, whereas mica is uncommon in the Hatay Graben and quartz concentrations are much lower (Boulton, 2006). This implies that the Hatay Graben was more distal from these detrital sediment sources than the Kırıkhan area. The quartz could have been eroded locally but there are no micaceous basement rocks in the vicinity suggesting that this material was transported from a greater distance. The nearest outcropping micaceous rocks are to the north of the suture zone, in the Berit region (described in detail by Robertson et al., 2006) some 150 km from the study area, there mica schists and granites outcrop. This suggests that by the Late Miocene, sediment eroded from north of the suture was being transported across the suture zone into the foreland basin that developed in front of the leading edge of the collision.

By contrast, to the south, in present day Syria, the main development of the Nahr El-Kabir half-graben took place in the Middle Miocene (Hardenberg and Robertson, 2007). There is a Late Serravallian thin chalk horizon present, but there are no sediments of Tortonian age present (Fig. 13). Hardenberg and Robertson (2007) explain this as due to local tectonics influencing sedimentation. Unlike the Hatay and Nahr El-Kabir areas, evidence for syn-sedimentary faulting has not been observed in Middle-Late Miocene sediments around Kırıkhan, Belen or Serinyol.

Messinian evaporites are not present in this area, although they have been identified to the north in the Iskenderun Bay (Boulton, 2006), in the Hatay Graben (Boulton et al., 2006; Boulton and Robertson 2007) and to the south in Syria (Hardenberg and Robertson, 2007). It is not clear whether evaporites were either not deposited in the area, were deposited and subsequently eroded, or are buried in the subsurface.

Pliocene sediments have not been identified around Kırıkhan, Belen or Serinyol, existing micropalaeontological dating indicates the youngest sediments near Serinyol are of Late Miocene age (Boulton et al., 2007). Pliocene sediments are present to the southeast in the Hatay Graben (Boulton et al., 2006) and to the south in the Nahr El-Kabir Graben (Hardenberg and Robertson, 2007) but both of these were tectonically active basins during the Neogene, whereas the Kırıkhan area was not. It is likely that regional Pliocene-Recent uplift, related to continued convergence between Arabia and Anatolia, induced terrestrial deposition earlier in the Kırıkhan-Karasu region, compared to areas to the south and west (Fig. 14e).

In addition to regional uplift, the DSFZ propagated northwards during the Pliocene. Transtension resulted in strike-slip and extensional components of deformation (Boulton, in review), the extensional component of deformation caused flank uplift and basin floor subsidence leading to the formation of the present topographic graben. The lack of dated Pliocene sediments and a Quaternary age for the rift fill suggests that significant topography did not develop until the Late Pliocene. Subsequently, up to ~350 m of Pleistocene river gravel (mostly unexposed) have accumulated within the Karasu Rift (Rojay et al., 2001). Moreover, some 11 inactive alluvial fans are interbedded with basalts that have yielded dates ranging from 1.57 – 0.05 Ma (Rojay et al., 2001; Yurtmen et al., 2002; Tatar et al., 2004). These basalts are associated with volcanic necks and have been attributed to block rotations and extension of the Karasu Rift (Tatar et al., 2004).

4.2 Timing of continental collision and implications

The Amanos Mountains are located at the westernmost interface between an extensive mobile belt to the east that has been deformed and uplifted following the closure of the southern Neotethys Ocean and consequent Arabia-Eurasia collision, and an extensive area to the west that has yet to undergo full continental collision (Mediterranean Basin). The study area is also located to the south of the Bitlis suture zone (Fig. 1). Constraining the timing of deformation, initial uplift and subsequent evolution of the southern Karasu Rift allows this area to be integrated into the broader geotectonic framework and enhances our understanding of the orogenic evolution in this sector of the Alpine-Himalayan chain.

In the East, south of the Zagros suture zone, collision has been shown to have commenced in the Late Eocene to Oligocene. Agard et al., (2005) constrained the timing of collision to between 35 and 25-23 Ma; after the last intrusion of mafic igneous material related to arc volcanism and prior to the onset of Late Oligocene/Early Miocene sedimentation. This is corroborated by the work of Hassami et al., (2001) on progressive unconformities in the Zagros that indicate deformation began in the Late Eocene. Further to the west in northern Iraq, terrestrial clastics dated to the Late Eocene have been inferred to represent sub-aerial uplift and erosion of the northeastern edge of the Arabian plate by this time (Dhannoun et al., 1988). Collectively, these data corroborate the findings from the Karasu Rift and Hatay Graben, where folded Eocene and older strata underlie an extensive hiatus of Oligocene indicating that compressional deformation along the north Arabian margin was taking place from the Late Eocene onwards.

Similarly, evidence from the north of the suture zone in the Caucasus and Caspian Basin indicates that the onset of collision also took place during the Late Eocene – Oligocene (Patton, 1993; Vincent et al., 2005; 2007) due to the presence of deformed and eroded Eocene strata unconformably overlain by clastics of presumed Oligocene age, olistostromes and compressional deformation observed in the subsurface. Late Eocene uplift has also been recorded in northern Iran (Alborz), where a Middle Eocene basin was inverted by the Early Oligocene (Alvavi, 1996; Guest et al., 2006).

In southern Turkey, north of the Bitlis suture zone, structural, sedimentological and stratigraphical studies have determined that the initial collision took place between the Late Eocene (Yilmaz, 1993) and Early Miocene time. Robertson et al., (2004; 2006) proposed that diachronous oblique subduction continued throughout the Eocene and that olistostromes indicate that the latest stages of subduction and initial collision took place in the Oligocene to Early Miocene. In many central Anatolian basins, sedimentation continued through the Late Eocene but was terminated by a basal Oligocene unconformity that is present in nearly all basins (e.g., Şarkişla basin, Gökten, 1986; Sivas basin, Dilek et al., 1999; Ulukisla basin, Clark and Robertson, 2005; Tuzgölü basin, Görür et al., 1989). In addition, latest Eocene folding is also reported for these same areas indicating that deformation propagated rapidly northwards into the interior of the Anatolian plate, as well as propagating rapidly northwards into the interior of the Eurasian Plate (Vincent et al., 2005; 2007). Alternatively, deformation initiation took place over a wide area.

The evidence present here, supports that from the region and shows that widespread deformation took place during the Late Eocene to Oligocene from Iran to western Anatolia. This indicates that the closure of the southern Neotethys and initial continental collision took place almost simultaneously along the entire frontal sector of the Arabian Plate with associated deformation propagating rapidly into the hinterland. This suggests that rather than the collision being diachronous in nature, it was broadly synchronous along the leading edge of the Arabian Plate.

Interestingly, the Eocene to earliest Oligocene was also a period of rapid expansion of the Antarctic continental ice sheet (Zachos et al., 2001); the closure of the Tethys Ocean in conjunction with other oceanographic changes, such as the widening of the North Atlantic Ocean (Zachos et al., 2001), would seem to be a significant factor in the climatic changes that occurred at the Eocene-Oligocene boundary.

5 Summary and Conclusions

Deposition of the Cenozoic sediments exposed in the Amanos Mountains, was dominantly controlled by subsidence related to continental collision taking place to the north and concomitant foreland basin formation south of the suture zone. The study area represents a Late Cretaceous to Eocene north-facing continental shelf at the southern Neotethys passive continental margin.. The Late Eocene to Oligocene is absent in the area due to erosion or non-deposition of sediments indicating that during some, if not all, of this period the area was uplifted and eroded. This uplift is attributed to the flexure of the crust and southward migration of the flexural bulge resulting from loading of the Arabian lithosphere due to continental closure of the Neotethys to the north. Recent research (e.g., Patton, 1993 Vincent et al., 2005; 2007; Allen and Armstrong, 2008) indicates that initial continental collision appears to have taken place nearly simultaneously along the leading edge of Arabia. Although, high resolution studies need to be undertaken to confirm this as the Late

Eocene to end Oligocene is a period of some 20 Ma and diachronism of the continental collision cannot be excluded completely.

Continental sedimentation during the Early Miocene reflects erosion of uplifted areas due to regional deformation resulting from the final closure of the Neotethys and suture tightening along the Misis-Andırın lineament. The flexural bulge passed to the south of the area and was shedding material northwards into the foreland basin; however, the proto-Amanos Mountains appear to already have developed into a topographic high and were additionally shedding sediment southwards. Marine transgression during the Middle to Late Miocene resulted in the deposition of localised patch reefs and clastic sediments were deposited into local depocentres (i.e., Hatay basin, Amik basin) with palaeocurrents directed to the south and west, indicating that the palaeoslope was orientated towards the developing Hatay Graben and not northwards towards the thrust front.

Regional uplift combined with a general regressive trend resulted in continental conditions by the latest Miocene/Pliocene that continue to the present day. Transtension, related to the northwards propagation of the DSFZ, resulted in the formation of the Karasu Rift during the Pliocene. The extensional component of deformation created accommodation space and fluvial conglomerates accumulated within the axial zone of the rift. These sediments are interbedded with lavas that resulted from localised extension and block rotations in the rift floor.

Acknowledgements

My thanks go to Malcolm Hart for foraminiferal identifications and to Alastair Robertson and Matthew Watkinson who commented on earlier versions of this manuscript. Additionally, the suggestions of the editor Gert Jan Weltje, Johan ten Veen and an anonymous reviewer greatly improved this manuscript. This work was initiated during a NERC PhD studentship at the University of Edinburgh and completed at the University of Plymouth with funding from the Royal Society.

References

Adiyaman, O., Chorowicz, J., 2002. Late Cenozoic tectonics and volcanism in the north western corner of the Arabian Plate: a consequence of the strike-slip Dead Sea Fault zone and the lateral escape of Anatolia. Journal of Volcanology and Geothermal Research, 117, 327-345.

Agard, P., Omrani, J., Jolivet, L., Mouthereau, F., 2005. Convergence history across Zagros (Iran): constrainsts from collisional and earlier deformation. International Journal of Earth Sciences, 94, 401-419.

Aktas, G., Robertson, A.H.F., l984. The Maden Complex, S E Turkey: evolution of a Neotethyan continental margin. In: Dixon, J.E., Robertson, A.H.F. (Eds.). The Geological Evolution of the Eastern Mediterranean. Geological Society, London, Special Publications, 17, 375-402.

Akyuz, H. S., Altunel, E., Karabacak, V., Yalciner C. C., 2006. Historical earthquake activity of the northern part of the Dead Sea Fault Zone, southern Turkey. Tectonophysics, 426 (3-4), 281-293.

Allen, M. B., Armstrong, H. A., 2008. Arabia-Eurasian collision and the forcing of mid Cenozoic global cooling. Palaeogeography, Palaeoclimatology Palaeoecology, doi: 10.1016/j.palaeo.2008.04.021

Alavai, M., 1996. Tectonostratigraphic synthesis and structural style of the Alborz mountain system in northern Iran. Journal of Geodynamics, 21, 1-33.

Al-Riyami, K., Robertson, A.H.F., Dixon, J.E, Xenophontos, C., 2002. Origin and emplacement of the Late Cretaceous Baer-Bassit ophiolite and its metamorphic sole in NW Syria, Lithos, 65, 225-260.

Arger, J., Mitchell, J., Westaway, R., 2000. Neogene and Quaternary volcanism of south-eastern Turkey. In: Bozkurt, E., Winchester, J. A., Piper, J. D. A. (eds). Tectonics and Magmatism of Turkey and the Surrounding Area. Geological Society, London, Special Publications, 173, 459-487.

Atan, O. R. 1969. Egribucak Kirikhan bölgesindeki ofiyolilerin jeolojisi ve petrografisi [Geology and Petrography of the Kirikhan District Ophiolite]. M.T.A yayini no 150, pp71, Ankara.

Beyarslan, M., Bingöl, A. F., 2000. Petrology of a super-subduction zone ophiolite (Elazığ Turkey). Canadian Journal of Earth Sciences, 37, 1411-1424.

Blair, T.C., McPherson, J.G., 1994. Alluvial fans and their natural distinction from rivers based on morphology, hydraulic processes, sedimentary processes, and facies assemblages. Journal of Sedimentary Research, A64, 450-489.

Boulton, S. J., Transpression or transtension? Structure of the northern Dead Sea Fault Zone. In review for Journal of Structural Geology.

Boulton, S. J., 2006. Tectonic-sedimentary evolution of the Cenozoic Hatay Graben, South Central Turkey. University of Edinburgh, unpublished PhD thesis, 414pp.

Boulton, S. J., Robertson, A. H. F., 2007. The Miocene of the Hatay area, S Turkey: Transition from the Arabian passive margin to an underfilled foreland basin related to closure of the Southern Neotethys Ocean. Sedimentary Geology, 198, 93-124.

Boulton, S. J., Robertson, A. H. F., Unlügenç, Ü. C., 2006. Tectonic and sedimentary evolution of the Cenozoic Hatay Graben, Southern Turkey: A two-phase, foreland basin then transtensional basin model. In: Robertson. A.H.F., Mountrakis, D. (eds.), Tectonic Evolution of the Eastern Mediterranean. Geological Society, London, Special Publications, 260, 613-634.

Boulton, S. J., Robertson, A. H. F., Ellam, R. M., Safak, Ü., Ünlügenç., U. C., 2007 Strontium isotopic and micropalaeontological dating used to redefine the stratigraphy of the Neotectonic Hatay Graben, southern Turkey. Turkish Journal of Earth Sciences, 16, 141-179.

Bouma, A. H., 1962. Sedimentology of some Flysch deposits: A graphic approach to facies interpretation, 168p, Elsevier, Amsterdam.

Bull, W. B., 1972. Recognition of alluvial fan deposits in the stratigraphic record. In: Rigby, J.K. & Hamblin, W. K. (eds) Recognition of ancient sedimentary environments. Society of Economic Palaeontology and Mineralogy Special Publication, 16, 63-83.

Çapan, U. Z., Vidal, P., Cantagrel, J. M., 1987. K –Ar, Sr and Pb isotopic study of Quaternary volcanism in the Karasu valley (Hatay), N-end of the Dead-Sea rift zone in SE-Turkey. Hacettepe University Earth Sciences, 14, 165-178.

Clark, M., Robertson, A., 2005. Uppermost Cretaceous – Lower Tertiary Ulukisla Basin, south central Turkey: sedimentary evolution of part of a unifed basin complex within an evolving Neotethyan suture zone. Sedimentary Geology, 173, 15 -51.

Çogulu, E., 1974. Ultrabasic tectonites and layered peridotites of the Hatay area (Turkey). Bulletin of the Maden Tektik Arama, 83, 139-147.

Dean, W. T., Krummenacher, R., 1961. Cambrian trilobites from the Amanos Mountains, Turkey. Palaeonotology, 4, 71-81.

Dean, W. T., Monod, O., Günay, Y., 1986. Lower Palaeozoic stratigraphy in the southern and central Amanos Mountains, south central Turkey. Geological Magazine, 123 (3), 215-226.

Delaloye, M., Piskin, Ö., Selçuk, H., Vuagnat, M. & Wagner, J-J. 1980. Geological section through the Hatay ophiolite along the Mediterranean coast, southern Turkey. Ofiliti, 52 (3), 205-216.

Dhannoun, H. Y., Aldabbagh, S. M. A., Hasso, A. A., 1988. The geochemistry of the Gercus Red-bed formation of Northeast Iraq. Chemical Geology, 69, 87-93.

Dilek, Y., Thy, P., Hacker, B., Grundvig, S., 1999. Structure and petrology of Tauride ophiolites and mafic dike intrusions (Turkey): implications for the Neotethyan ocean. Geological Soceity of America Bulletin, 111, 1192– 1216.

Dokumaci, Y., 1997. Belen tektono-stratigrafik incelemesi (Tectono-stratigraphic investigations of the Belen area). MSc. Thesis, University of Çukurova.

Dubertret, L. 1939. Sur la genèse et l'ãges des roches vertes syriennes. Comptes Rendus de l'Academie des Sciences, Paris, 209 P763.

Dubertret, L. 1953. Géologie des roches vertes du nord-ouest de la Syrie et du Hatay (Turquie). Notes et Mémoires sur le Moyen-Orient, Museum Nationale et histoire naturelle, 5, 5-179, Paris.

Franseen, E. K., Esteban, M., Ward, W. C., Rouchy, J-M., 1996. Models for carbonate stratigraphy from Miocene reef complexes of Mediterranean regions. Society for Sedimentary Geology – Concepts in Sedimentology and Paleontology Volume 5, 391pp

Garfunkel, Z., Ben-Avraham, Z., 1996. The structure of the Dead Sea Basin. Tectonophysics, 255, 155-176.

Garfunkel, Z., Zak, I., Freund, R., 1981. Active Faulting in the Dead Sea Rift. Tectonophysics, 80, 1-26.

Gökten, E., 1986. Palaeocene carbonate turbidites of the Şarkişla region, Turkey—their significance in an orogenic basin. Sedimentary Geology 49, 143– 165.

Görür, N., Tüysüz, O., Şengör, A.M.C., 1998. Tectonic evolution of the Central Anatolian Basins. International Geological Review, 40, 831–850.

Guest, B., Stockli, D. F., Grove, M., Axen, G. J., Lam, P. S., Hassanzadeh, J., 2006. Thermal histories from the central Alborz Mountains, northern Iran: Implications for the spatial and temporal distribution of deformation in northern Iran. Geological Society of America Bulletin, 118, 1507 – 1521.

Gül, M., 2006. Evolution of the turbidite system in the Kahramanmaras Basin. Cükürova University, Unpublished PhD thesis.

Günay, Y. 1984. Amanos daglarinin jeolojisi ve Karasu-Hatay grabeninin petrol olanaklari. TPAS Hakkari-Saryaj Projesi, TPAO-1984, Ankara.

Hall, R., 1976. Ophiolite emplacement and evolution of the Taurus suture zone. South-east Turkey. Geological Society of America, Bulletin, 87, 1078-1088.

Hardenberg, M., Robertson, A.H.F., 2007. Sedimentology of the NW margin of the Arabian plate and the SW-NE-trending Nahr El-Kabir half-graben in northern Syria during latest Cretaceous-Cenozoic. Sedimentary Geology. Doi: 10.1016/j.sedgeo.2007.02.009

Hempton, M. R., 1987. Constraints on Arabian Plate motion and extensional history of the Red Sea. Tectonics 6, 687-705.

Hessami, K., Koyi, H. A., Talbot, C. J.,Tabasi, H., Shabanian, E., 2001. Progressive unconformities within an evolving foreland fold-thrust belt, Zagros Mountains. Journal of the Geological Society, London, 158, 969 – 981.

Heward, A.P., 1978. Alluvial fan sequence and mega sequence models: with examples from Westphalian D-Stephanian B coalfields, northern Spain. In: Maill, A.D. (ed) Fluvial Sedimentology. Canadian Society of Petroleum Geologists, Memoirs, 5, 669-702.

Holmes, A. 1965. Principles of Physical Geology, 2nd Edition. Nelson, London. Pp 1288.

Ishmawi, R., 1972. Geologie des nordlichen Mittelteils des Amanos-Gebirges zwischen Islahiye und Bahçe (S. Türkei). Geotektonischen Forschungen, 42, 34-63.

Janetzko, P., 1972. Geologische Untersuchungen an der Ostflanke des sudlichen Amanos-Gebirges zwischen Islahiye und Hassa (Sudtürkei). Geotektonischen Forschungen, 42, 3-33.

Karig, D. E., Kozlu, H., 1990.Late Palaeogene – Neogene evolution of the triple junction region near Maraş, south central Turkey. Journal of the Geological Society, London, 147, 1023-1034.

Kelling, G., Gökcen, S. L., Floyd, P. A., Gökcen, N., 1987. Neogene tectonics and plate convergence in the eastern Mediterranean: New data from southern Turkey. Geology, 15, 425-429.

Kop, A., 1996. Kirikhan ve Kuzeyinin tektono-stratigrafik incelemesi (Tectono-stratigraphic investigations of Kirikhan and its northern area). MSc Thesis, University of Çukurova, Turkey.

Kozlu, H. 1982. İskenderun Baseni Anadolu nun Kambrien teşekkülleri ve bunların Doğu İran Kambrieni ile mukayesesi. MTA periodical no 66, Ankara.

Kozlu, H., 1997. Tectono-stratigraphic units of the Neogene basins (Iskenderun, Misis-Andirin) and their tectonic evolution in the eastern Mediterranean region. [PhD Thesis] Natural Science Institute, Cukurova University, Turkey.

Lahner, L., 1972. Geologische Untersuchungen an der Ostflanke des des mittleren Amanos (SE Türkei). Geotektonischen Forschungen, 42, 64-96.

Lyberis, N., 1988. Tectonic evolution of the Gulf of Suez and the Gulf of Aqaba. Tectonophysics, 153 (1-4), 209-220.

Miall, A. D., 1978. Fluvial Sedimentology. Canadian Society of Petroleum Geologists Memoir, 5, 859pp.

Miall, A. D., 1985. Architectural element analysis: a new method of facies analysis applied to fluvial deposits. Earth-Science Reviews, 22, 261-308.

Miall, A. D., 1996. The Geology of Fluvial Deposits: Sedimentary facies, basin analysis and petroleum geology. Springer-Verlag, Berlin, 582 pp.

Miller, K. G., Kominz, M. A., Browning, J. V., Wright, J. D., Mountain, G. S., Katz, M. E., Sugarman, P. J., Cramer, B. S., Christie-Blick, N., Pekar, S. F., 2005. The Phanerozoic record of global sea-level change. Science, 310 (5752), 1293-1298.

Meulenkamp, J. E., Sissingh, W., 2003. Tertiary palaeogeography and tectonostratigraphic evolution of the Northern and Southern Peri-Tethys platforms and the intermediate domains of the African-Eurasian convergent plate boundary zone. Palaeogeography, Palaeoclimatology, Palaeoecology, 196, 209-228.

Myrow, P.M., Southard, J.B., 1996. Tempestite deposition. Journal of Sedimentary Research, 66 (5), 875-887.

Neale, J.W., 1988. Ostracods and palaeosalinity reconstruction. In: De Deckker, P. Colin, J.-P., Peypouquet, J.P., (Eds), Ostracoda in the Earth Science, Elsevier, Amsterdam, pp. 125–155.

Nilsen, T. H., 1982. Fluvial Models. In: Sandstone Depositional Environments, Ed. P.A. Scholl & D. Spearing. pp115-137. AAPG Memoir 31.

Orton, G.J., 1988. A spectrum of Middle Ordovician fan deltas and braidplain deltas, North Wales: a consequence of varying fluvial clastic input. In: Nemec, W., Steel, R.J. (Eds) Fan Deltas: Sedimentology and Tectonic Settings. Blackie, London, 23-49.

Över, S., Ünlügenç, U. C., Bellier, O., 2002. Quaternary stress regime change in the Hatay region, SE Turkey. Geophysics Journal International, 148, 649-662.

Parlak, O., Kop, A., Ünlügenç, U. C., Demirkol, C., 1998. Geochronology and geochemistry of basaltic rocks in the Karasu graben around Kirikhan Hatay, S. Turkey. Turkish Journal of Earth Sciences, 7, 53-61.

Patton, D.K., 1993. Samgori field, Republic of Georgia: critical review of island-arc oil and gas. Journal of Petroleum Geology, 16, 153-167.

Piskin, O., Delaloye, M., Selçuk, H., Wagner, J., 1986. Guide to Hatay Geology SE Turkey. Oflioliti, 11, 87-104.

Postma, G., 1986. Classification for sediment gravity-flow deposits based on flow conditions during sedimentation. Geology, 14, 291-294.

Postma, G., 1990. Depositional architecture and facies of rivers and fan deltas: a synthesis. In: Collela, A., Prior, D.B., (Eds) Coarse-grained deltas. Special Publication of the International Association of Sedimentologists, 10, 13-27.

Reading, H. G. & Collinson, J. D. 1996. Clastic coasts. In: Sedimentary Environments: Processes, Facies and Stratigraphy, 3rd edition Ed: H.G. Reading. Blackwell Science. 154-231.

Robertson, A. H. F., 1998. Mesozoic-Tertiary Tectonic evolution of the easternmost Mediterranean area: integration of marine and land evidence. In: Robertson, A. H. F., Emeis, K.-C., Richter, C., Camerlenghi, A. (eds.), Proceedings of the Ocean Drilling Program, Scientific Results, 160, 723-782.

Robertson, A.H.F., 2000. Mesozoic-Tertiary tectonic-sedimentary evolution of a south Tethyan oceanic basin and its margins in southern Turkey. In: Bozkurt, E., Winchester, J.A, Piper., J.D. (eds)., Tectonics and Magmatism in Turkey and the Surrounding Area.. Geological Society, London, Special Publications, 173, 43-82.

Robertson, A.H.F., 2002. Overview of the genesis and emplacement of Mesozoic ophiolites in the Eastern Mediterranean Tethyan region, Lithos, 65, 1-67.

Robertson, A. H. F, Dixon, J. E., 1984. Introduction: aspects of the geological evolution of the Eastern Mediterranean. In: Dixon, J.E., Robertson, A. H. F (eds). The Geological evolution of the Eastern Mediterranean. Geological Society , London, Special Publications, 17, 1-74.

Robertson, A. H. F., Ünlügenç, U. C., Inan, N., Tasli, K. 2004. The Misis-Andirin Complex: a Mid-Tertiary melange related to late-stage subduction of the Southern Neotethys in S Turkey. Journal of Asian Earth Sciences, 22, 413-453.

Robertson, A. H. F., Ustaömer, T., Parlak, O., Ünlügenç, U. C., Taşlı, K., İnan, N., 2006. The Berit transect of the Tauride thrust belt, S Turkey: Late Cretaceous – Early Cenozoic accretionary/collisional processes related to closure of the Southern Neotethys. Journal of Asian Earth Sciences, 27, 108-145.

Rojay, B., Heimann, A., Toprak, V., 2001. Neotectonic and volcanic characteristics of the Karasu fault zone Anatolia, Turkey: The transition zone between the Dead Sea transform and the East Anatolian fault zone. Geodynamica Acta, 14, 197-212.

Rosenfeld, A., Hirsch, F., 2005. The Paleocene – Eocene of Israel. In: Hall, J. K., Krasheninnikov, V. A., Hirsch, F., Benjamini, C., Flexer, A. (eds). Geological Framework of the Levant, Volume II: The Levantine Basin and Israel. Historical Productions – Hall, Jerusalem. 437-459.

Saller, A., Armin, R., Ichram, L.O., Sulliven, C., 1993. Sequence stratigraphy of aggrading and backstepping carbonate shelves, Oligocene, Central Kalmantan, Indonesia. In: Loucks, R. G., Sarg, J. F. (eds), Carbonate Sequence Stratigraphy: Recent developments and Applications. American Association of Petroleum Geologists Memoir, 57, 267-290.

Şaroğlu, F., Emre Ö., & Kusçu, İ. 1992. The East Anatolian fault zone of Turkey. Annales Tectonicae, 6, 99-125.

Şengör, A.M.C., Yılmaz, Y., 1981. Tethyan evolution of Turkey: a plate tectonic approach. Tectonophysics, 75, 81-241.

Schwan, W., 1971. Geology and tectonics of the central Amanos Mountains. In: Cambell, A.S (ed) Geology and History of Turkey. Tripoli: The petroleum Exploration Society of Libya, 283-303.

Sharland, P.R., Casey, D.M., Davies, R.B., Simmons, M.D., Sutcliffe, O.E., 2004. Arabian Plate stratigraphy-revisions to SP2. GeoArabia, 9, 199-214.

Tatar, O., Piper, J. D. A., Gürsoy, H., Heimann, A., Koçbulut, F., 2004. Neotectonic deformation in the transition zone between the Dead Sea Transform and the East Anatolian Fault Zone, Southern Turkey: a palaeomagnetic study of the Karasu Rift volcanism. Tectonophysics, 385, 17-43.

Vincent, S. J., Allen, M. B., Ismail-Zadeh, A. D., Flecker, R., Foland, K. A., Simmons, M. D., 2005. Insights from the Talysh of Azerbaijan into the Paleogene evolution of the South Caspian region. Geological Society of America Bulletin, 11, 1513 – 1533.

Vincent, S. J., Morton, A. C., Carter, A., Gibbs, S., Barabadze, T. G., 2007. Oligocene uplift of the Western Greater Caucasus: an effect of initial Arabia-Eurasia collision. Terra Nova, 19, 160-166.

Westaway, R., 2003. Kinematics of the Middle East and Eastern Mediterranean updated. Turkish Journal of Earth Sciences, 12, 5-46.

Westaway, R., Arger, J., 2001. Kinematics of the Malatya-Ovacik fault zone. Geodynamica Acta, 14, 103-131.

Wright V. P & Burchette, T. P. 1996. Shallow water carbonate environments. In: Sedimentary Environments: Processes, Facies and Stratigraphy, 3rd edition Ed: H.G. Reading. Pp. 325-394. Blackwell Science.

Yılmaz, Y., Yiğitbaş, E., Genç, S. C., 1993. Ophiolitic and metamorphic assemblages of southeast Anatolia and the significance in the geological evolution of the orogenic belt. Tectonics, 12, 1280-1297.

Yurtmen, S., Guillou, H., Westaway, R, Rowbotham, G., Tatar, O., 2002. Rate of strike-slip motion on the Amanos Fault (Karasu Valley, southern Turkey) constrained by K-Ar dating and geochemical analysis of Quaternary basalts. Tectonophysics, 344, 207-246.

Zachos, J. C., Pagani, M., Sloan, E. T., Billups, K., 2001. Trends, rhythms, and aberrations in global climate 65 Ma to present. Science, 292, 686-694.

Tables

Name	Age	Lithology	Boundaries	Thickness
Gökdere Fm	Tortonian - Messinian	Marl and litharenite	Conformable with Kepez Fm or unconformable on or faulted against older units. Upper boundary to younger sediments not exposed.	400 – 700m
Kepez Fm	Langhian	Wackestone and packstone	Lower boundary unconformable on Kıcı or conformable with Gökdere, upper transitional to Gökdere Fm.	15m
Kıcı Fm	Aquitanian – Burdigalian	Conglomerates, litharenites and mudstones	Unconformable with units above and below. Also fault contacts with Gökdere Fm	100 - 150m
Hacıdağ Fm	Palaeocene - Eocene	Calcarenite, wackestone, packstone and rudstone	Base conformable with Cona and Esmisek Fms unconformable on the ophiolitic complex. Angular unconformity with Kıcı and Gökdere Fms. Faulted contacts with other formations numerous.	> 400m

Table 1. Summary of the characteristics of the lithostratigraphic units discussed in the text.

	Serinyol	Kan1	Kan2	Kan3	Gok 1	Gok 2	Gok 3	Gok 4
Serpentinite	0	0	27	10	95	80	33	40
Chert	14	9	12	2	0	0	3	2
Algal lmst	73	0	0	0	0	0	0	0
Chert + lmst	13	20	26	21	0	0	0	0
Bioclastic lmst	0	5	12	13	0	0	0	0
Nummul. lmst	0	0	0	0	0	0	4	1
Undiff lmst	0	74	42	35	5	20	5	0
Total	100	108	119	81	100	100	45	43

Table 2. Clast counts from conglomerate horizons at Serinyol (Ser), Kanlidere (Kan) and Gökdere (Gok), location of sites shown on figures 6 and 9. The clast count was undertaken by drawing a 1x1 m grid upon the outcrop, 10 cm intersections were marked and the clast at each intersection counted, giving the clast composition of ~ 100 clasts at each location.

Sample No	SB73A	SB71A	SB77A	SB94A	SB142A
Age	L.Mio	L. Mio	L. Mio	U.Mio	U. Mio
S.Calcite	20	31	37.5	28.5	19.5
Micrite	2	1.5	10.5	6.5	7
Qtz(m)	1	7.5	0	10.5	5.5
Qtz(p)	1.5	6.5	0	10	11.5
Ophiolite	51.5	7	48.5	13.5	11.5
bioclast	0	0	1	2	0
mica	0	0.5	0	2	0
carbonate	5.5	19	1.5	12.5	30
siliciclastic	14.5	17	0.5	8	6
feldspar	0	1	0	4	0.5
opaque	4	4	0	2.5	2
other	0	5	0.5	0	6.5
Total	100	100	100	100	100

Table 3. Point-counting results for sandstones. Two hundred points were counted for each thin-section in order to have a statistically meaningful sample group. For locations of samples (SB73A, etc.) see Fig. 1. S.Calcite = sparry calcite; Qtz (m) = monocrystalline quartz; Qtz (p) = polycrystalline quartz.

Sample	Age	Fm.	Quartz	Calcite	Smectite	Clinochrysotile	Albite	Dolomite	Muscovite	Others	Total
SB72A	U.Mio	G	29	51	0	0	12	2	0	6	100
SB95A	U.Mio	G	28	49	0	0	0	2	5	16	100
SB98A	U.Mio	G	14	57	0	8	2	0	16	3	100
SB140A	U.Mio	G	15	56	0.1	22	5	0	0	1.9	100
SB135A	U.Mio	G	38	59	0	3	0	0	0	0	100
SB137A	U.Mio	G	26	57	0	0	10	0	6	1	100
SB104A	L.Mio	K	32	41	0	0	10	0	0	17	100
SB76A	L.Mio	K	20	5	16	39	0	0	20	0	100
SB126A	Eocene	H	17	61	0	1	0	0	14	7	100
SB128A	Eocene	H	20	78	0	0	2	0	0	0	100
SB133A	Eocene	H	19	79	0	0	2	0	0	0	100

Table 4. XRD determinations of fine-grained sediments (sample locations shown on Fig. 1). Two samples were analysed from the Kıcı Formation (SB76A & SB104A), both have compositions rich quartz and clinochrysotile. Sample SB76A contains abundant smectite (16%) and muscovite (20%) but low calcite (5%). Sample SB104A, by comparison, has no smectite or muscovite but has a high (56%) calcite content. Six samples were analysed from the Gökdere Formation. All have significant amounts of quartz (14-38%) and high calcite (31-78%) contents. Albite and muscovite also are relatively abundant. Formation codes; G = Gökdere; K = Kıcı and H = Hacıdağ.

1033 **Figures**

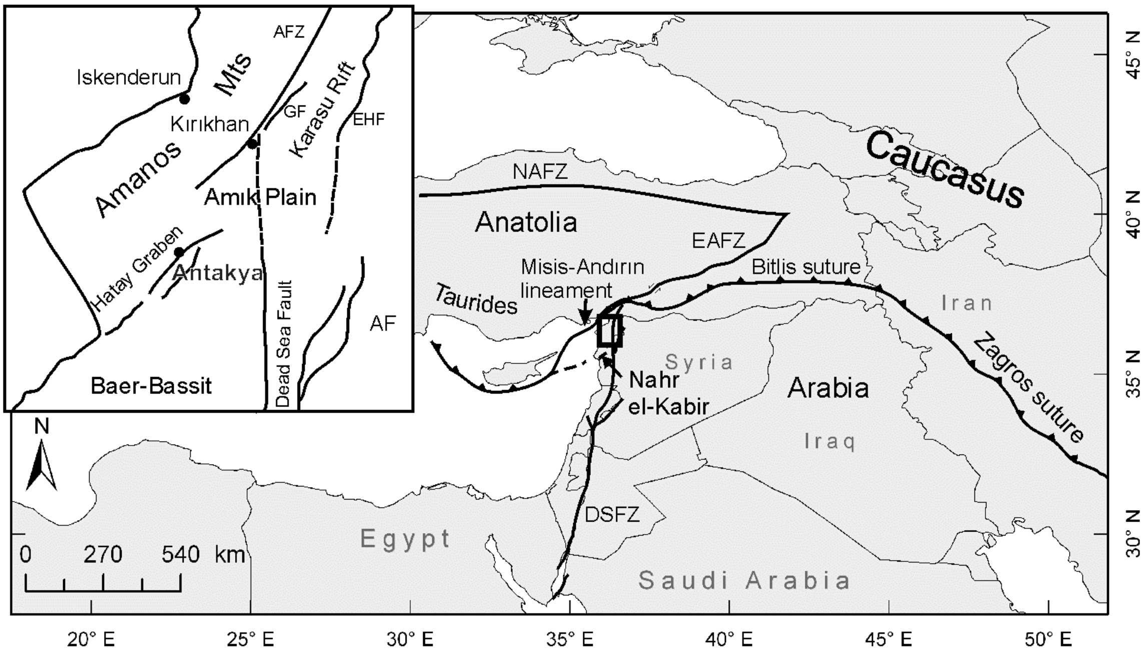

1034

1035 Figure 1. Regional geodynamic framework, small box shows location of the study area. Inset box
1036 shows major faults of the study area and locale, DSFZ: Dead Sea Fault Zone; EAFZ, East Anatolian
1037 Fault Zone; NAFZ, North Anatolian Fault Zone; AFZ, Amanos Fault Zone, EHF, East Hatay Fault;
1038 AF, Afrin Fault; GF, Guzelce Fault.

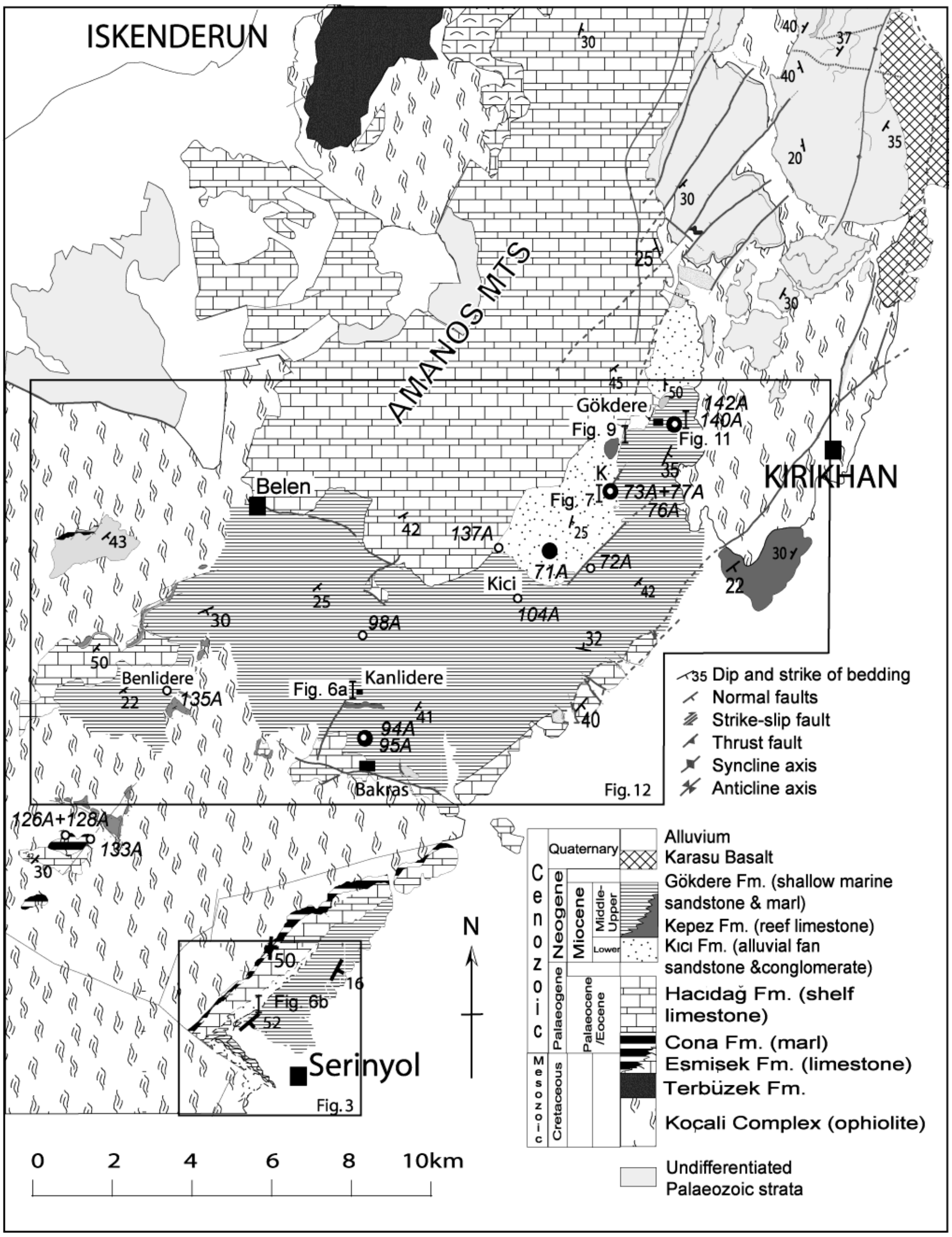

Figure 2. Geological map of the northern part of the study area around the towns of Kırıkhan and Belen, showing the main places discussed in the text and the locations of samples used in petrological analysis (modified from Boulton et al., 2007); black circles indicate locations where sandstones for point-counting were collected, white circles indicate locations where fine-grained sediments were taken for XRD analysis, bars with appended Figure numbers indicate locations of logs, while boxes indicate the extent of figures 3 and 13. The letter K indicates the location of the type section of the Kıcı Formation at Kurtisoğuksu.

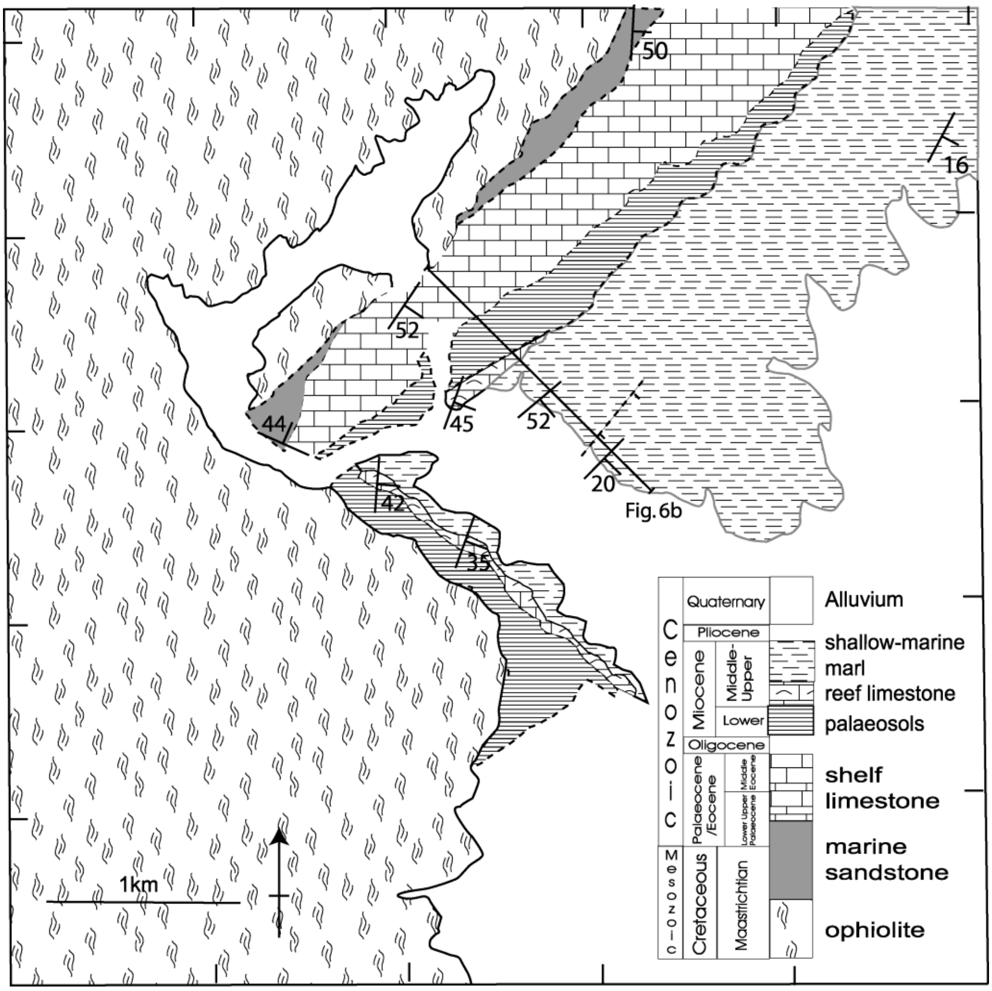

Figure 3. Geological map of the area around Serinyol, see figure 2 for the location within the Karasu Rift. Black line indicates the location of the log shown in figure 6b. Note the town of Serinyol is located under the key.

Figure 4a. Incipient slump in thin-bedded Eocene limestone at 0255391/4036316 (Map sheet Antakya P36-a2), north of the Kırıkhan-Antakya road; b). Isoclinal recumbent slump fold observed in Eocene limestones (circled compass-clinometer provides scale) just off the main Belen road at grid ref. 0252481/4041026 (Map sheet Antakya P36-a2). Orientations of this fold hinge and the incipient slump shown in (a) deomstrate that the palaeoslope was inclined to the north (see fig. 5 for bedding data); c). General view of the Eocene sediments near Serinyol at 0248123/4029755 (Map sheet Antakya P36-a3). Three units can be observed the basal unit is ophiolite (Op), an erosive unconformity separates the basement from the overlying Eocene composed of a basal conglomerate (Con) and upper bedded limestones (Lm) above; d). View of the Eocene (Ha - RHS) – Lower Miocene (Kı - LHS) boundary near the village of Gökdere, along which a stream has flowed. Eocene limestones are folded, while the overlying Kıcı formation is unfolded, dipping southeastwards (towards the camera). The Lower Miocene strata is formed of a basal algal boundstone representing a brief marine incursion, with continental clastics above.

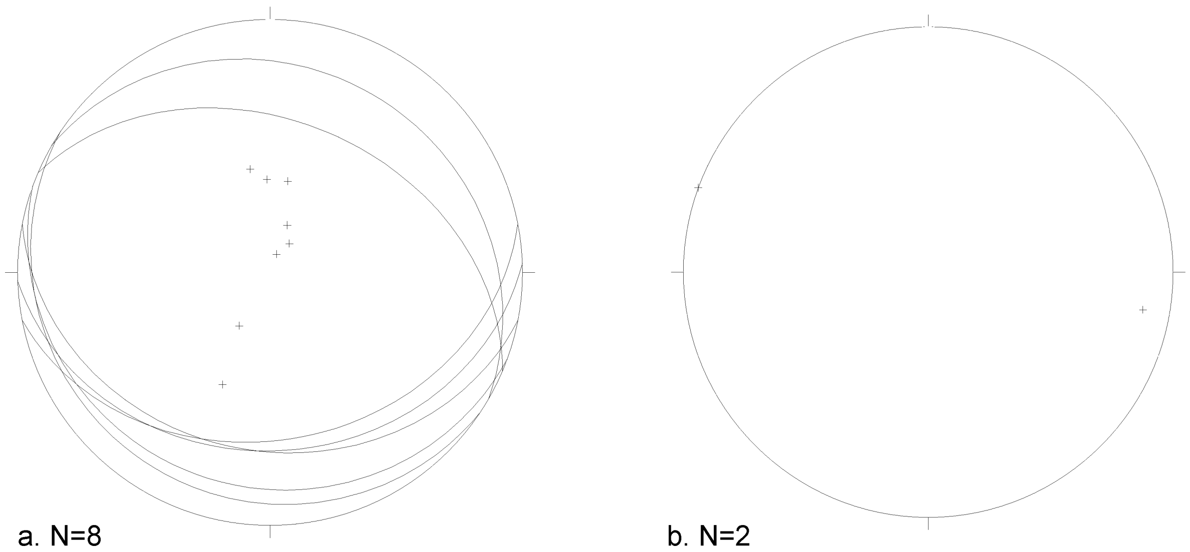

Figure 5a). Bedding plane data (shown as great circles and pole to plane - the crosses) for limbs of slump folds observed in the Eocene Hacıdağ Formation; b). Crosses indicate orientation of hinge lines of measured slump folds (Fig. 4b). Both sets of data indicate the general orientation of the palaeoslope was N to NNE; perpendicular to the hinges of the folds that form parallel to the strike of the palaeoslope.

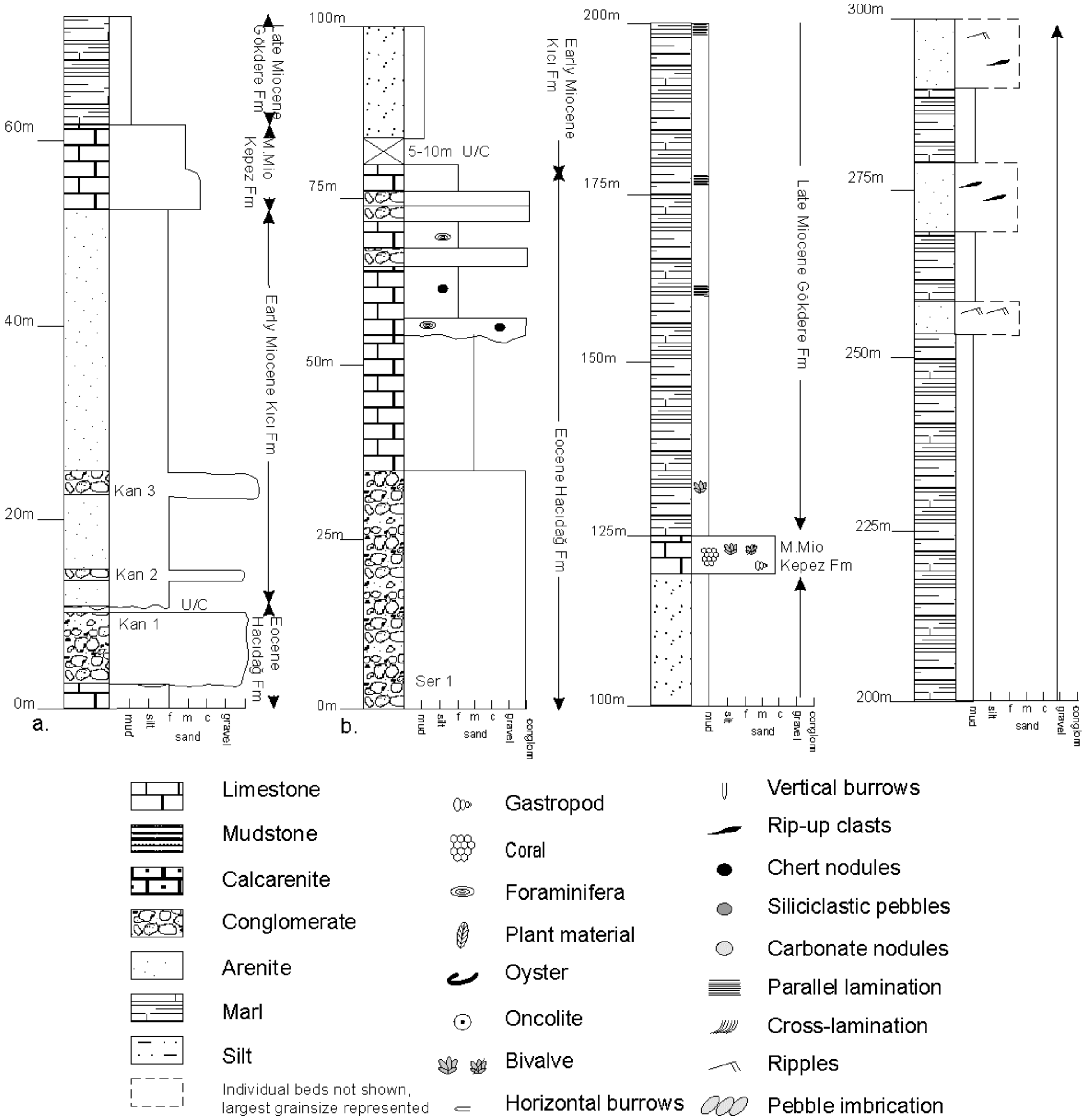

Figure 6a). Log of Sediments at Kanlidere (on figure 2). Kan1, 2, 3 and Ser 1 show the positions where conglomerate clast counts were undertaken, see Table 2 for results; b. Log of sediments at Serinyol (see figure 3 for position of logged section). Key for all logs shown at the bottom.

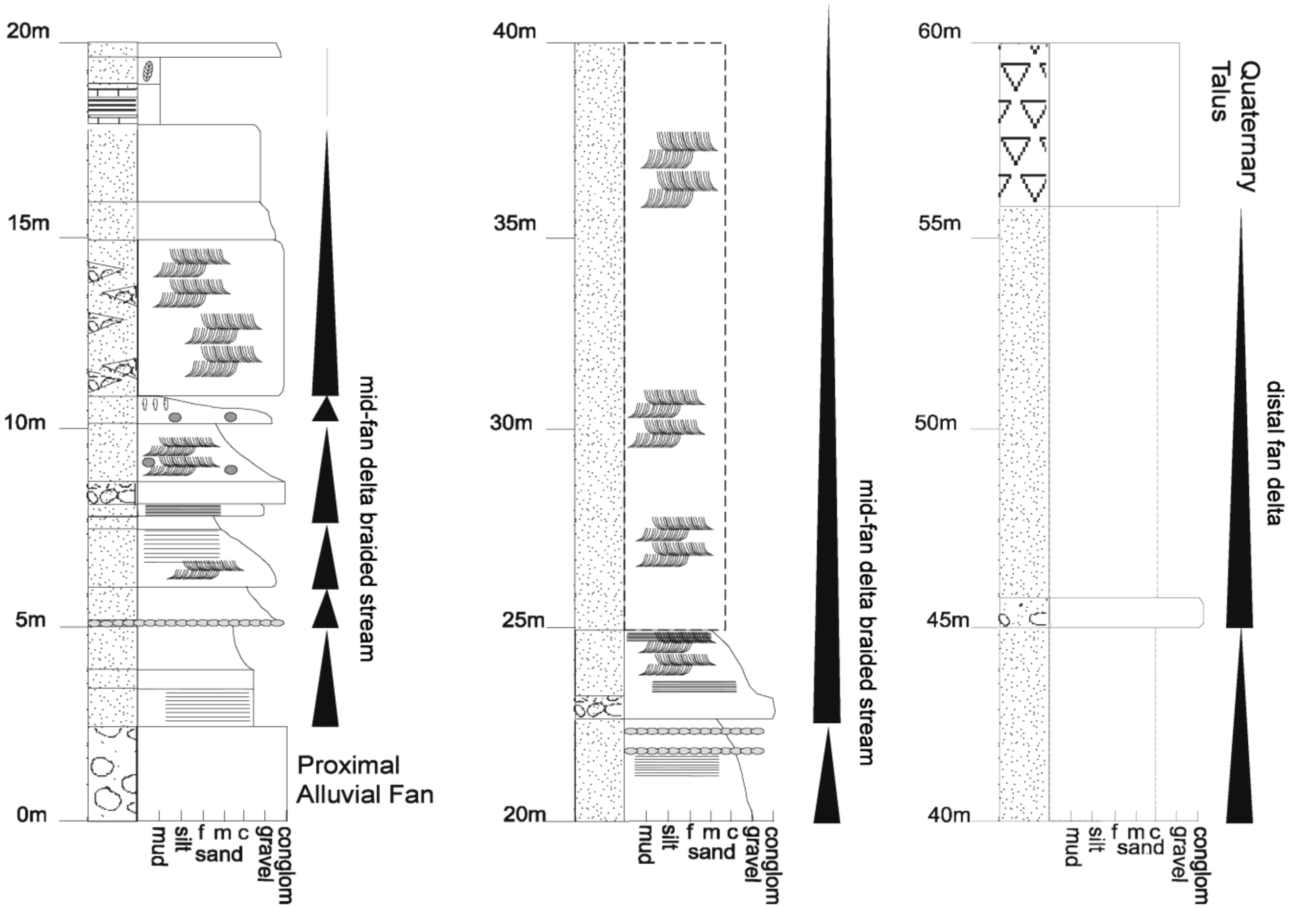

Figure 7. Log of Kıcı formation at the type section (K; Fig. 2) with sedimentary environments and fining-upwards cycles shown. Fining-upwards sequences may represent bar processes or where a basal conglomerate is present, may be a channel fill deposit (modified from Boulton et al., 2007). See figure 6 for key.

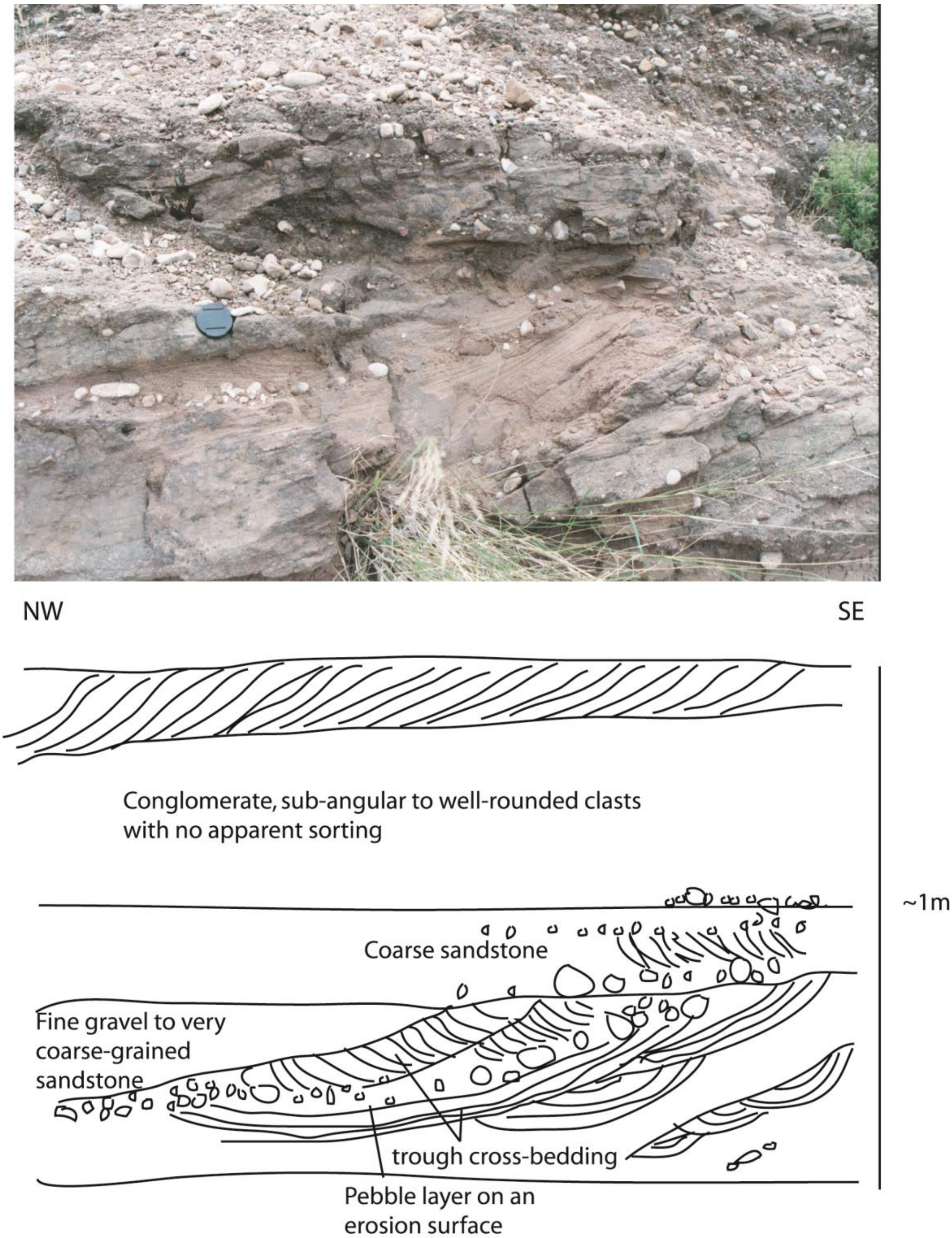

Figure 8. Field photograph and sketch of cross-bedded sandstones typical of the Kıcı Formation, from the type section (K; Fig. 2). See figure 6 for key.

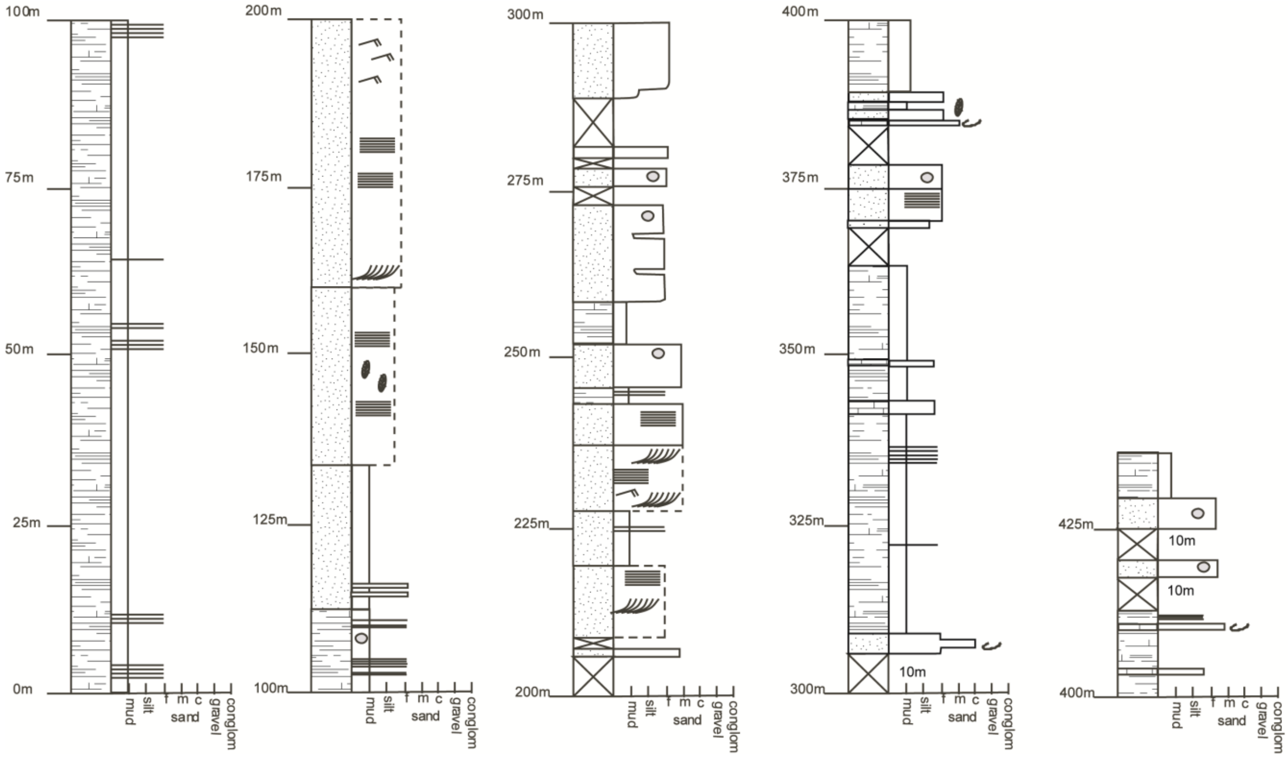

Figure 9. Log of the Kıcı Formation near the village of Gökdere (Fig. 2), the sequence is interpreted as an alluvial fan deposit where coarsening-upwards cycles possibly represent progradation of individual fan lobes. Gok 1, 2, 3, 4 refer to locations where conglomerate clast counts were undertaken, results shown in table 2.

Figure 10a. Close up of a conglomerate horizon in the Kıcı Formation, at Kanlidere, note borings in limestone clasts; b). Close-up of blocks of coralline limestone from the Kepez Formation observed near Serinyol; c). View over the village of Gökdere with part of Cenozoic sedimentary sequence exposed from left to right in the foreground. In the lower left the ophiolite complex (Op) is observed, above is the Upper Miocene Gökdere Formation (Go) dipping southeastwards (to the right). The Middle Miocene Kepez Formation (Ke) can be observed as a laterally discontinuous outcrop exposed in the side of hill (in the centre of the field of view), the Kıcı Formation is not present at this location; d). View of the middle of the Gökdere Formation at the type section showing a typical sand-body on the left hand side.

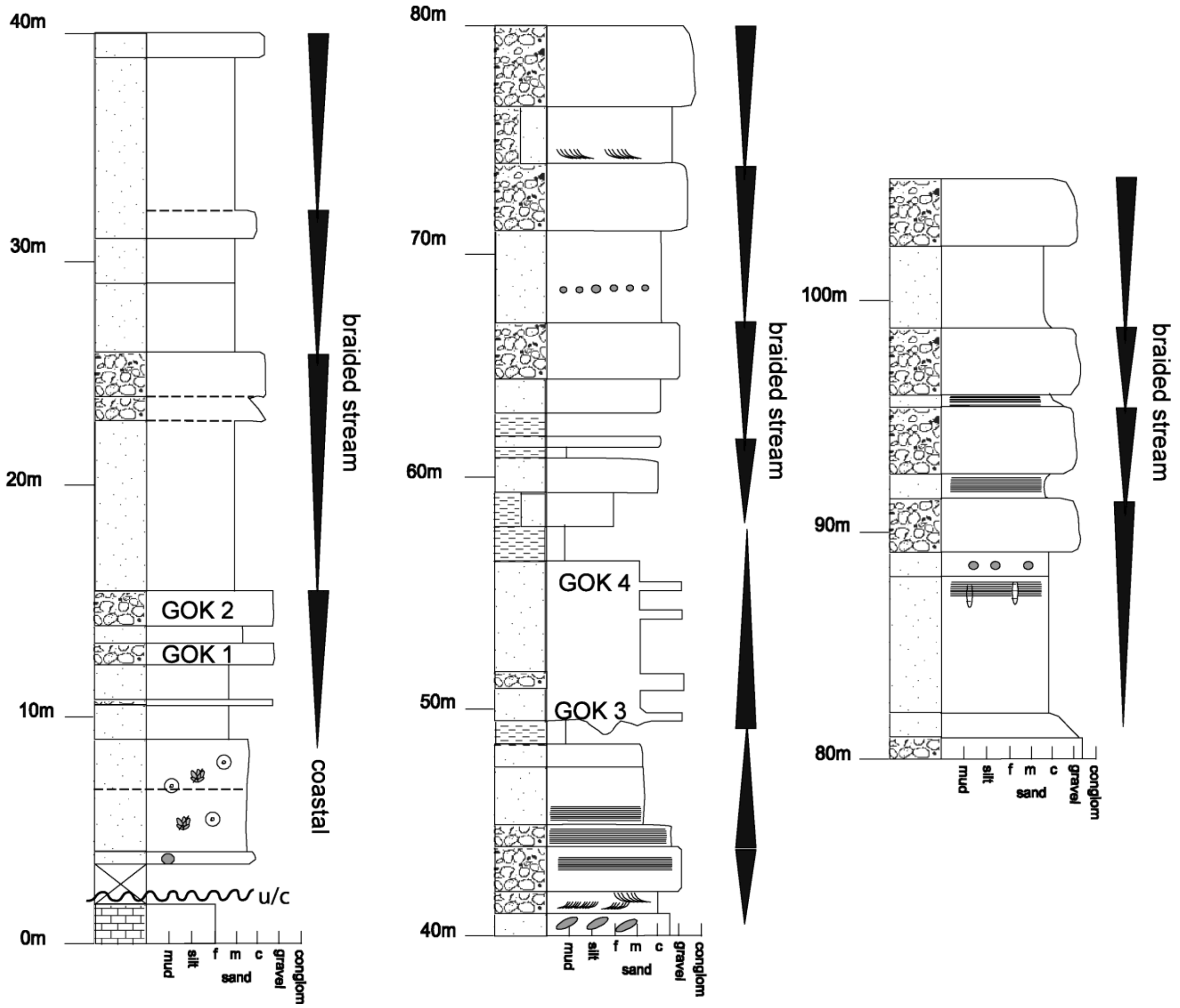

1106

1107 Figure 11. Log of the Gökdere Formation at Gökdere (Fig. 2). See figure 6 for key. The sequence is

1108 interpreted as a regressive shallow-marine sequence.

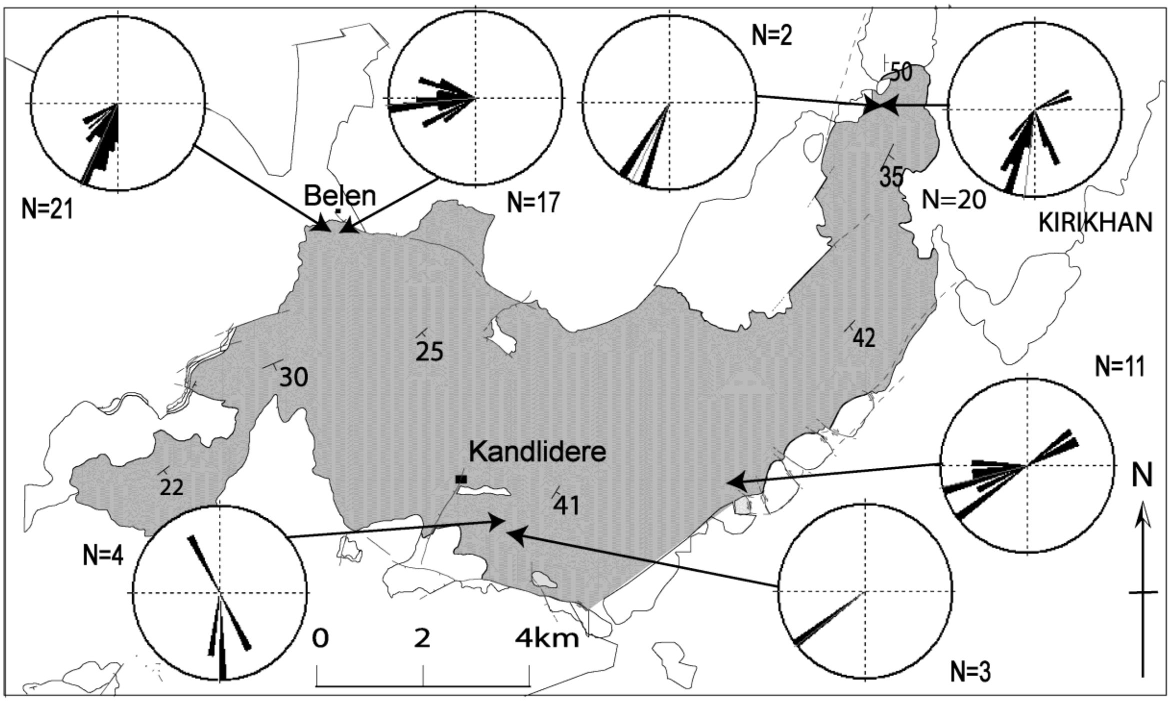

Figure 12. Rose diagrams of measured palaeocurrents from the Upper Miocene Gökdere Formation in the central part of the study are (extent of this map shown on figure 2). N = No. of measurements at each locality.

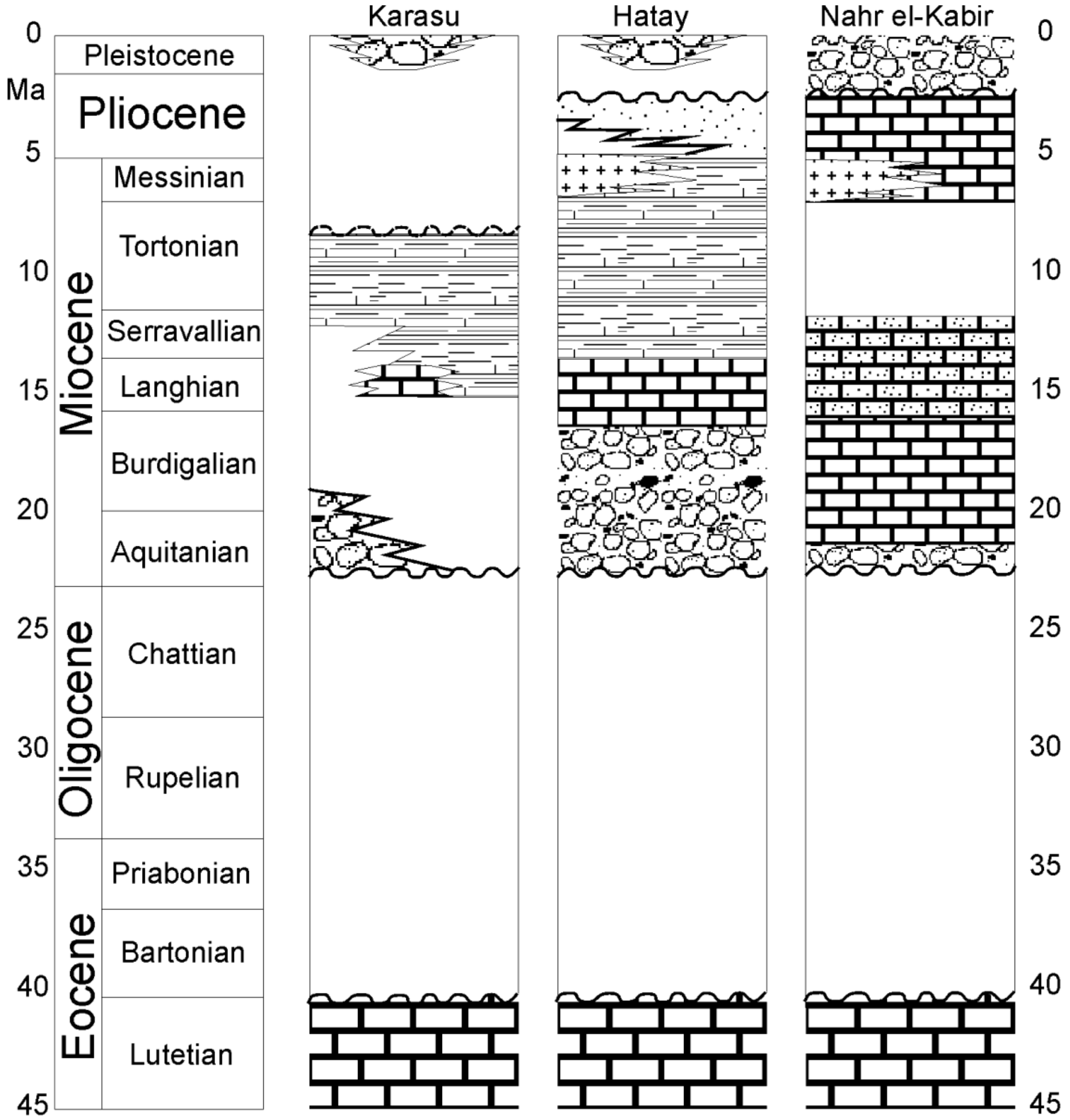

Figure 13. Stratigraphic columns showing the stratigraphy of the Karasu Rift, Hatay Graben and Nahr el-Kabir Graben (locations of areas shown on Figure 1). Note the similarities between the Karasu Rift and adjacent Hatay Graben and the differences of both areas to the Nahr el-Kabir Graben to the south. See figure 6 for key.

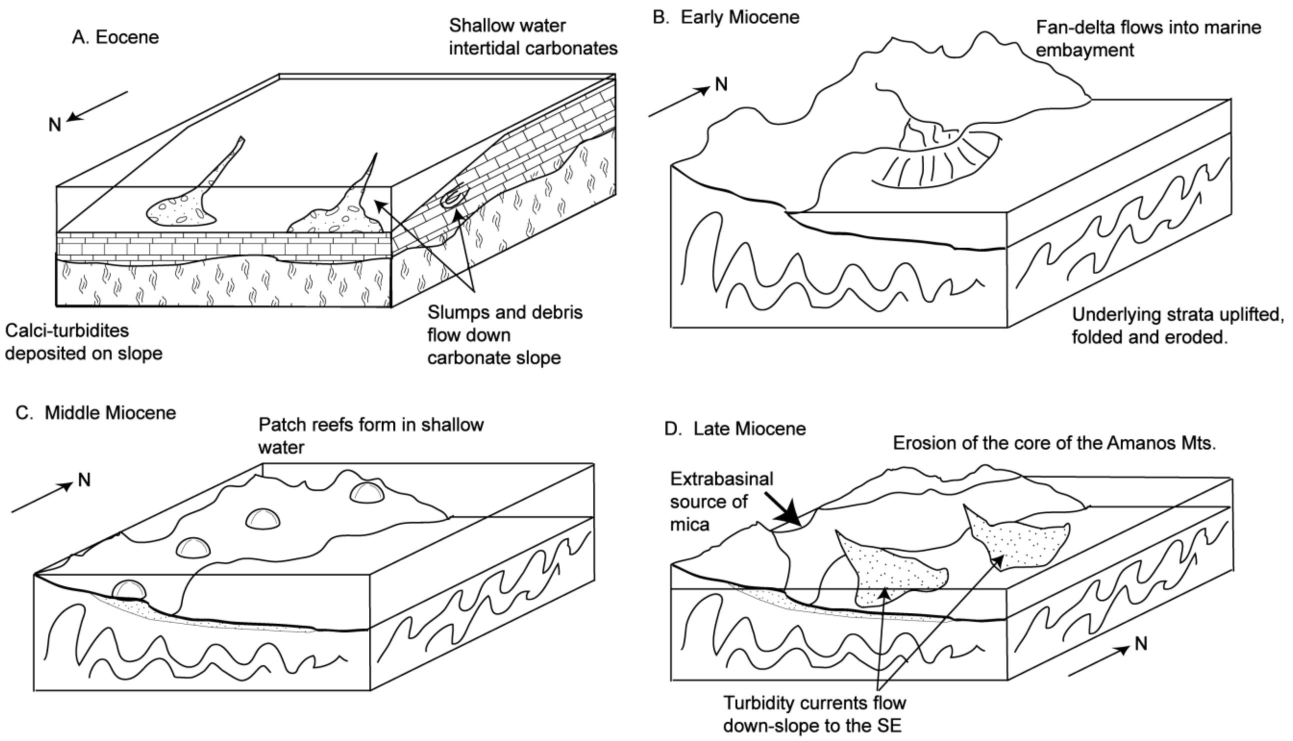

Figure 14. Block diagrams illustrating inferred palaeogeographical conditions during A) Eocene; B) Lower Miocene; C) Middle Miocene; D) Upper Miocene and E) Pliocene to Recent times. N.B. Note the reversed orientation of diagram (A).